

SEP 5 1981

567

(NASA-CR-173511) DEVELOPMENT OF GREAT LAKES  
 ALGORITHMS FOR THE NIMBUS-G COASTAL ZONE  
 COLOR SCANNER Final Report (Environmental  
 Research Inst. of Michigan) 95 p  
 HC A05/MF A01

N84-27258  
 Unclass  
 13545

CACL 05B G3/43

150000-11-F

Phase I - Final Technical Report

# DEVELOPMENT OF GREAT LAKES ALGORITHMS FOR THE NIMBUS-G COASTAL ZONE COLOR SCANNER

FRED J. TANIS AND DAVID R. LYZENGA  
Applications Division

JUNE 1981



NASA/Lewis Research Center  
NAS3-22442  
Cleveland, Ohio 44135  
Technical Monitor: Thom A. Coney

ENVIRONMENTAL  
**RESEARCH INSTITUTE OF MICHIGAN**  
 BOX 8618 • ANN ARBOR • MICHIGAN 48107

REPORT DOCUMENTATION PAGE		READ INSTRUCTIONS BEFORE COMPLETING FORM
1. REPORT NUMBER 150000-11-F	2. GOVT ACCESSION NO.	3. RECIPIENT'S CATALOG NUMBER
4. TITLE (and Subtitle) Phase I - Final Technical Report DEVELOPMENT OF GREAT LAKES ALGORITHMS FOR THE NIMBUS-G COASTAL ZONE COLOR SCANNER	5. TYPE OF REPORT & PERIOD COVERED Final Technical Report 4/1/80-2/28/81	
	6. PERFORMING ORG. REPORT NUMBER 150000-11-F	
7. AUTHOR(s)  Fred J. Tanis and David R. Lyzenga	8. CONTRACT OR GRANT NUMBER (s)  NAS3-22442	
9. PERFORMING ORGANIZATION NAME AND ADDRESS Environmental Research Institute of Michigan Applications Division Ann Arbor, Michigan 48107	10. PROGRAM ELEMENT, PROJECT, TASK AREA & WORK UNIT NUMBERS	
11. CONTROLLING OFFICE NAME AND ADDRESS NASA/Lewis Research Center Cleveland, Ohio 44135 Technical Monitor: Thom A. Coney - Mail Stop MS-542	12. REPORT DATE June 1981	
	13. NUMBER OF PAGES vi + 90	
14. MONITORING AGENCY NAME AND ADDRESS (if different from Controlling Office)	15. SECURITY CLASS. (of this report) Unclassified	
	15a. DECLASSIFICATION/DOWNGRADING SCHEDULE	
16. DISTRIBUTION STATEMENT (of this Report)		
17. DISTRIBUTION STATEMENT (of the abstract entered in Block 20, if different from Report)		
18. SUPPLEMENTARY NOTES		
19. KEY WORDS (Continue on reverse side if necessary and identify by block number) Water Reflectance Models Geometric Polyconic Image Projection Optical Proportion Atmospheric Algorithms		
20. ABSTRACT (Continue on reverse side if necessary and identify by block number) The Great Lakes Experimental Team (GLET) has conducted a series of experiments in the Great Lakes designed to evaluate the application of Nimbus-G Coastal Zone Color Scanner (CZCS). Absorption and scattering measurement data were reduced to obtain a preliminary optical model for the Great Lakes. Available optical models were used in turn to calculate subsurface reflectances for expected concentrations of chlorophyll-a pigment and suspended minerals.		

20. ABSTRACT (Continued)

Multiple non-linear regression techniques were used to derive CZCS water quality prediction equations from Great Lakes simulation data. An existing atmospheric model was combined with a water model to provide the necessary simulation data for evaluation of preliminary CZCS algorithms.

A CZCS scanner model was developed which accounts for image distorting scanner and satellite motions. This model was used in turn to generate mapping polynomials that define the transformation from the original image to one configured in a polyconic projection.

## PREFACE

This final report as issued by the Applications Division of the Environmental Research Institute of Michigan (ERIM) under National Aeronautics and Space Administration (NASA) contract NAS3-22442 for the Lewis Research Center (LeRC) covers the contract period from April 1, 1980 through February 28, 1981. The technical representative for the contract officer was Mr. Thom A. Coney of LeRC. The Principal Investigator was Fred J. Tanis with important contributions to the technical program made by David R. Lyzenga, Glenn Davis, and Robert Dye. This research was conducted by the Applications Division under the direction of Mr. Donald S. Lowe.

This contract involves developing algorithms to map selected constituent concentrations in Great Lakes waters from the Coastal Zone Color Scanner (CZCS). The approach is based upon the inherent optical characteristics of Great Lakes waters.

A number of institutions and universities are involved in the project and are organized as the Great Lakes Experimental Team (GLET). This report covers ERIM's activities in the project during Phase I of an anticipated two phase program.

## TABLE OF CONTENTS

PREFACE	iii
LIST OF FIGURES	v
LIST OF TABLES	vi
1. INTRODUCTION	1
1.1 Statement of the Problem	1
1.2 Project Goals and ERIM Tasks	2
1.3 Project Background	3
1.4 Summer 1980 Great Lakes Experiments	4
2. DEVELOPMENT OF A GEOMETRIC CORRECTION ALGORITHM FOR CZCS	7
2.1 Investigation of Regression Model Techniques	8
2.2 Coastal Zone Color Scanner Model	9
2.3 Generation of Mapping Polynomials	10
2.4 Resampling of the CZCS May 8, 1979 Imagery	11
3. USE OF OPTICAL MODELS TO DEVELOP CZCS CHLOROPHYLL AND SUSPENDED SEDIMENT ALGORITHMS	17
3.1 Applicability of Existing Algorithms	17
3.2 Optical Models and Radiative Transfer Theory	19
3.2.1 Optical Models	19
3.2.2 Radiative Transfer Theory	21
3.3 Preliminary Analysis of Optical Properties for the Great Lakes	23
3.4 Discussion of Atmospheric Effects and Corrections	32
3.5 Preliminary CZCS Water Algorithms	38
4. SUMMARY AND CONCLUSIONS	49
REFERENCES	51
APPENDIX A: CZCS GEOMETRIC CORRECTION SOFTWARE	53

## LIST OF FIGURES

<u>FIGURE</u>	<u>TITLE</u>	<u>PAGE</u>
1a&b	Original and Polyconic Projected CZCS Thermal Band Images of the Great Lakes For May 8, 1979.	13
2	Results from the Lake Erie Settling Experiment.	31
3	Subsurface reflectance (percent) at CZCS wavelengths (443 nm, 520 nm, 550 nm, 670 nm) as predicted by the Lake Ontario 5-component model [18].	39
4	Subsurface reflectance (percent) at CZCS wavelengths (443 nm, 520 nm, 550 nm, 670 nm) as predicted by the Lake Ontario 4-component model [18].	40
5	Subsurface reflectance (percent) at CZCS wavelengths (443 nm, 520 nm, 550 nm, 670 nm) as predicted by the Preliminary 1980 Optical Model.	41
6	Projected subsurface reflectances (percent) as predicted by each of the above reflectance models.	44
7	Great Lakes CZCS Image for May 8, 1979 Reconstructed from Water and Land Files.	48

## LIST OF TABLES

<u>TABLE</u>	<u>TITLE</u>	<u>PAGE</u>
1	Ground Control Locations.	15
2	Optical Cross Sections for Great Lakes Water Quality Model	26
3	Optical Measurements made During Settling Experiment	30
4	Extinction Coefficients Calculated from MIE Scattering Theory	33
5	First Principal Components Derived from CZCS Satellite Measured Radiances	37

## INTRODUCTION

The Great Lakes Experimental Team (GLET) is conducting a series of experiments in the Great Lakes region designed to evaluate the application of the Nimbus G Coastal Zone Color Scanner (CZCS). Potential uses foreseen include assessment of trophic status, verification and spatial refinement of whole lake models, and observation of temporal and spatial dynamics of phytoplankton. Currently members of the NOAA Nimbus Experimental Team (NET) are developing chlorophyll and sediment algorithms largely to be applied, to the open ocean [1]. Preliminary examination of these algorithms indicates they have limited applicability to the Great Lakes. Concentrations and compositional differences of suspended materials along with atmospheric aerosol variants are expected to exhibit important differences from the marine environment and result in additional complexities. The focus of the present program is the development and testing of atmospheric and water algorithms appropriate to the Great Lakes as well as evaluation of existing algorithms developed for the marine environment.

## 1.1 STATEMENT OF THE PROBLEM

The quantification of substances in Great Lakes waters by satellite visible radiometry is dependent on a thorough understanding of the radiative transfer processes in the atmosphere, at the waters surface, and in the water column itself. It has been well established that the content of water, be it particulate or dissolved substances affects the apparent color. By sensing color with a high signal to noise ratio in narrow spectral bands CZCS provides a means of looking at the water content which has been heretofore unavailable from satellite data. Since the air and water effects are coupled to the CZCS radiometric data, removal of atmospheric effects becomes critical to the success of



the Great Lakes verification. Once removed the radiance which is scattered upward from beneath the surface can be observed clearly by the satellite. Effectively the radiance reaching the satellite from the lake surface amounts to only five percent of the total radiation and consequently ninety-five percent of the radiation received is from atmospheric backscatter and surface reflectance. Furthermore, the variation in radiance at the satellite due to change in constituent concentration are on the order of one percent while the variation due to atmospheric changes can be considerably higher. The spatially varying atmospheric component is due principally to aerosol scattering. The significance of the atmospheric problem for a water target has been demonstrated by Hovis and Lung [2] and more recently by Quenzel and Kaestner [3] who compared the variability of the atmosphere with the reflected light from phytoplankton suspensions. Thus unless atmospheric effects can be negated resolving quantitative information on water constituents it is considered to be most difficult. Baring elimination of the atmospheric effects the water problem requires understanding how the inherent optical properties relate to the measured quantities of chlorophyll-a pigment, phytoplankton cell count, suspended solids, and dissolved organics. Previous algorithms relied heavily on the availability of extensive surface truth [4,5,6]. For this study algorithms are sought which can be based on optical properties specific to the Great Lakes and which reduce the present requirements for extensive surface truth.

## 1.2 PROJECT GOALS AND ERIM TASKS

In order to be acceptable to the Great Lakes user community CZCS algorithms must, in our estimation, meet at least two general criteria. First, the algorithms must be able to predict accurately surface concentrations of chlorophyll-a pigments and suspended sediment over widely varying ranges and do so with little or no ancillary measurement data. Second, they must be capable of making predictions over water masses

which exhibit spatial variation in atmospheric haze and surface concentration.

The ERIM participation in the Great Lakes experiments involves two phases. The first covers the period from April 1980 through February 1981 and is the subject of this report. This first phase has involved development of computer software to process CZCS tapes received from the NASA Goddard Space Flight Center (GSFC), collection of surface truth measurement data in connection with CZCS overflights of the Great Lakes, and formulation of preliminary algorithms. The second phase will involve development and testing of specific atmospheric and water computer algorithms for CZCS. The water algorithms will be based upon radiative transfer theory and measured optical properties of Great Lakes waters. Existing atmospheric models will be tested, including some recently developed models, using surface truth and low altitude aircraft measurements made during the 1980 GLET experiments. These models in turn will be utilized in the development of operational algorithms for removing atmospheric effects from CZCS data without the direct use of a large number of in situ measurements of atmospheric optical depth. Our approach is to remove spatially variable components using properties of the data itself. It is anticipated that both the algorithm development by Gordon [7] and that by a group at the Scripps Institute of Oceanography [8] will be tested for their suitability to the Great Lakes atmospheric environment.

### 1.3 PROJECT BACKGROUND

The scientific objective of CZCS is to determine water constituents quantitatively and to carry out such measurements over large areas which are not possible or practical to be obtained with surface ship investigations. Currently the Nimbus experimental team (CZCS-NET) is investigating CZCS capabilities to quantify material suspended or dissolved in the water. These validation studies are concentrating on the ocean

environment. The present study is similar in design to the NET investigations but the focus is on a freshwater environment. A number of institutions, research centers, and universities plan to participate various aspects of the program. In addition to LeRC, which has led the current effort, participants in the Great Lakes Experiment include ERIM, Canada Center for Inland Waters, NOAA Great Lakes Environmental Research Laboratory, EPA Grosse Ile, University of Minnesota, University of Wisconsin, and others. These participants have a wide variety of backgrounds and capabilities which can be applied to the project. While it is understood that LeRC will not be able to participate fully in subsequent program phases it is anticipated that they will maintain an active interest in the project and promote the continuity of the GLET.

#### 1.4 SUMMER 1980 GREAT LAKES EXPERIMENTS

During 1980 a number of surface truth measurements were made coincident with CZCS overflights of the Great Lakes. Experiments were conducted at three principal locations in the Great Lakes: western Lake Erie, Duluth area of western Lake Superior, and the Grand Haven area in Lake Michigan. All of these experiments were designed to gather necessary validation data and optical properties specific to the Great Lakes waters. Measurements made included the following:

- (1) Aircraft flights were made by NASA LeRC F-106 aircraft fitted with the Ocean Color Scanner at altitudes of 500 and 41,000 feet.
- (2) Water samples were gathered by the University of Michigan GLRD and the NOAA GLERL and subsequently analyzed for chlorophyll pigments and suspended solids.
- (3) NASA LeRC made various surface ship radiometric measurements.

- (4) NASA Langley Research Center deployed a mobile optical laboratory to Cleveland. Optical parameters including absorption, beam attenuation, and scattering were measured on selected water samples.
- (5) The Naval Oceans System Center conducted in-situ submersible radiometer measurements of subsurface downwelling and upwelling irradiance at selected sites in Lake Erie.

A total of twenty separate sites were sampled in the Great Lakes, fourteen of which were made in connection with CZCS overflights. Only a very small portion of the above measurements have been analyzed to date but all analyses are expected to be completed in phase II of the program.

DEVELOPMENT OF A GEOMETRIC CORRECTION  
ALGORITHM FOR CZCS

The objective of this task was the modification of existing software and the development of a new scanner model which together will permit transformation to CZCS line and pixel coordinates into earth latitude and longitude. CZCS scanning geometry including variable tilt angle for Great Lakes viewing was combined with ground control points to derive the appropriate transformation matrix. Landsat geometric processing programs were adapted and modified as necessary to process available CZCS taped data for the Great Lakes. The initial accuracy goal was set to one pixel in each direction. In this task our efforts included investigation of geometric correction based on the 77 tie points per line, development of a CZCS scanner model, generation of mapping polynomials, modification of resampling software, and processing of an example image.

The geometric correction of an image results from two operations. First, mapping polynomials are generated that define the transformation from the raw original image to the corrected image. Second, the corrected image is created from the uncorrected image using these mapping polynomials. Two fifth-order, twenty-one term polynomials were used in this process, one for each dimension of the image. These polynomials define the transformation which makes the corrected image conform to a given map projection as well as adjust for viewing distortions such as satellite position, satellite motion, and earth motion. Two approaches were considered in the present study; a geometric regression analysis approach, and an orbit modelling approach. Both of these approaches are based on extensive experience with Landsat image correction. Thus the basic techniques were extended in the present effort to accommodate the Coastal Zone Color Scanner.

## 2.1 INVESTIGATION OF REGRESSION MODEL TECHNIQUES

Regression analysis was undertaken as the first approach to geometric correction. While this approach is considered to be straightforward it has the disadvantage of requiring extensive ground control points which makes it time consuming. In order to get satisfactory results, fifty or more points should be taken for each scene. The first image considered was taken on November 8, 1978. An image analyst selected forty-six ground control points of which forty-one were found to be suitable. A geometric regression analysis of these points produced mapping polynomials which could predict the location of these points with standard errors of 517 meters in the horizontal dimension and 553 meters in the vertical direction. Since the pixel size of the CZCS is nominally 825 by 825 meters, derived mapping polynomials are estimated to be accurate to within one pixel. These results are comparable to those typically obtained with Landsat processing.

Selecting ground control points is a lengthy process so an alternative method was sought to correct the scene. An attempt was made to use the ephemeris data that accompanies each image tape. Specifically, anchor points are included that describe the geographic position at 77 locations on each scan line. A two hundred point sample distributed throughout the scene was selected for testing. Geometric regression of these points showed errors greater than 13,000 meters in both dimensions. A similar set of points selected from a second scene taken on May 8, 1979 produced errors of the same magnitude. Subsequent to this experiment we learned that later versions of the GSFC processing algorithm had improved the accuracy of the anchor points considerably. Fortunately, we were able to obtain a copy of the May 8 scene with the improved anchor point values. However, this image was the only one available under the new version [9] and thus it was used exclusively for purposes of testing the geometric correction algorithms. A geometric regression was performed on a 429 point sample of anchor points which was in turn used to produce a set of mapping polynomials. Using the

mapping polynomials derived from the anchor points the ground control points were predicted with RMS errors of 4068 meters in the horizontal dimension and 4425 meters in the vertical dimension. This five pixel accuracy is within that claimed by GSFC for the anchor point reference system. Geometric regression of a set of sixty-two ground control points taken from the same image showed errors of 557 meters in the horizontal and 893 meters in the vertical.

An attempt was made to obtain additional scenes with which to verify these results. Two scenes were obtained from the Lewis Research Center for this purpose. The first, April 17, 1979 had extensive cloud cover and it was impossible to obtain an adequate number of ground control points. The second, June 20, 1979 was centered in an area east and south of Lake Erie. Most of the image covered the Atlantic Ocean and again ground control points in the Great Lakes area were insufficient.

## 2.2 COASTAL ZONE COLOR SCANNER MODEL

The scanner model developed for CZCS is based upon our experience with Landsat and in its present form takes each image control point in turn and projects it to the earth's surface. The line number for each point is used to interpolate for the latitude, longitude, and altitude from the values supplied with the tape reference data for each scene. The point number is used to calculate the mirror scan angle, which together with the reported tilt angle determines the scanner line-of-sight vector in spacecraft coordinates.

A series of rotations through the angles of roll, pitch, heading, latitude, and longitude plus a translation provide the transformation to earth centered coordinates. The intersection of the line-of-sight vector with the surface of the spheroid is then derived and converted to latitude and longitude. These coordinates are compared with the corresponding values obtained from map data, and the discrepancies minimized by successive refinement of the estimated roll, pitch, and heading. The

present model permits manual intervention with the operator who can supply needed refinements to the latitude and longitude parameters. It is anticipated that future model versions will eliminate the need for operator interaction and model adjustments.

Once unsatisfactory control points have been eliminated the refined attitude and location data are combined with the model. The cartographic projection is then selected and subjected to polynomial regression analysis which yields in turn the coefficients to a pair of twenty-one term, fifth degree polynomials. These polynomials provide an approximating transformation from cartographic coordinates to the original image coordinates.

The uses to which a scanner model of the imaging system for the CZCS are twofold. First, the image control points and their corresponding map control points may be easily evaluated for consistency with other points and any outliers rejected. Second, the coefficients for global mapping polynomials used in the resampling process can be derived by a fit to the model rather than to the points themselves. This feature permits the use of a much smaller number of points than would be needed for simple regression.

### 2.3 GENERATION OF MAPPING POLYNOMIALS

An arbitrary set of points were selected from the test image and used together with the scanner model to derive a set of mapping polynomials. A number of scanner variables including satellite attitude and position will influence the model results. Values of latitude and longitude are converted to line and pixel location in the resulting image via the equations that define the desired map projection.

The process used to resample a corrected image works in the reverse direction. For each pixel location in the resulting image the program calculates the corresponding location in the original image. This process implies reversing the projection equations in order to derive



the desired latitude and longitude information. However, operation of the scanner model in reverse so as to select original pixel locations which correspond to given location in the corrected image is most difficult and unwieldy. Alternatively, the pair of twenty-one term polynomials is generated to satisfy this mapping requirement. One polynomial describes the east-west position and the other the north-south location. The selected arbitrary image points mentioned above are used to generate coefficients for each term in the polynomial. The complete set of coefficients defines the mapping from the original image to the correct projected image.

Mapping coefficients are generated by step-wise regression in which the correlation matrix is calculated relating each term to its ability to predict the location of the point in the original image. A regression coefficient is calculated for the most influential term. This term is in turn removed from the matrix and the step regression continued until all terms that contribute predictive capability are included in the coefficient matrix. By utilizing points selected throughout the image file derived mapping coefficients are applicable over the entire pixel range in the corrected image. RMS errors are also calculated by the polynomial generation software for predicted locations in the original image. In the resampling process the correct image line and pixel number is translated to a location in the original image. The nearest neighbor pixel is then copied to the corrected image file.

#### 2.4 RESAMPLING OF THE CZCS MAY 8, 1979 IMAGERY

Using the scanner model software fifty-four ground control points of the May 8, 1979 Great Lakes image file were tested for consistency with model parameters. Results indicated north-south RMS errors of 693 meters and east-west errors of 1338 meters respectively. Based upon existing satellite attitude information the scanner model was used to generate latitude and longitude positions from which the appropriate polynomial coefficients could be derived. The polynomial prediction

errors were found to be 55 meters in the north-south direction and 583 meters in the east-west direction. Combining these results leads to an expected total error of 748 meters in the north-south and 1921 meters in the east-west or approximately 1.0 and 2.5 pixels, respectively in the original image. Figure 1 shows the original and resampled images for the Great Lakes portion of the CZCS data file. This area includes all of the lakes except Lake Superior and the upper most portions of Lakes Huron and Michigan which are included in the next CZCS data frame.

Unfortunately portions of Lakes Michigan and Huron are obscured by cloud cover. Lakes Erie and Ontario are essential cloud free with the exception of a thin covering over the western basin of Lake Erie. The resampled image was made using a polyconic projection and an arbitrary pixel size of 500 by 500 meters. So as to verify the accuracy of the corrected image twenty additional ground control points were selected and compared to those predicted by the projection polynomials. Table 1 shows the results of this comparison. The maximum difference occurred for the sixth test point which was found to be 3000 meters in the north-south direction and 7500 meters in the east-west direction. Test pixels located near the center of the original image and principal meridian showed, on the other hand, minimal errors. For example the second test pixel had a north-south error of 500 meters and an east-west error of 2500 meters. The mean error was estimated to be 200 meters in the north-south direction and 1875 meters in the east-west direction. A listing of CZCS geometric correction programs developed for the PDP-11/70 computer facility are contained in Appendix A.



Original CZCS Image

Figure 1a. Original and Polyconic Projected CZCS Thermal Band Images of the  
Great Lakes for May 8, 1979.



Polyconic Projected Image

Figure 1b. Original and Polyconic Projected CZCS Thermal Band Images of the Great Lakes for May 8, 1979.

TABLE 1  
GROUND CONTROL LOCATIONS

Location	Predicted		Actual		Difference	
	Row	Column	Row	Column	Row	Column
Toledo, Ohio	1028	1274	1029	1278	1	4
Detroit, Michigan	808	1182	806	1191	-2	9
Detroit, Michigan	843	1122	841	1131	-2	9
Flint, Michigan	692	1381	690	1390	-2	9
Flint, Michigan	688	1163	685	1174	-3	9
Tawas City, Michigan	311	1150	305	1165	-6	15
Cleveland, Ohio	1039	1564	1039	1567	0	3
Erie, Pennsylvania	801	1495	801	1500	0	5
Buffalo, New York	731	1806	731	1808	0	2
Buffalo, New York	865	1827	865	1829	0	2
Toronto, Ontario	646	1788	647	1793	1	5
Toronto, Ontario	658	1895	659	1897	1	2
Toronto, Ontario	563	1804	563	1808	0	4
Elmira, New York	785	2204	786	2203	1	-1
Elmira, New York	715	2308	715	2307	0	-1
Rochester, New York	635	2129	636	2129	1	0
Rochester, New York	462	2290	463	2290	1	0
Kingston, Ontario	438	2103	439	2103	1	0
Kingston, Ontario	365	2321	365	2321	0	0
Kingston, Ontario	419	2222	419	2221	0	-1
Mean Difference					-0.41	3.75
Standard Deviation					1.79	4.44

## USE OF OPTICAL MODELS TO DEVELOP CZCS CHLOROPHYLL AND SUSPENDED SEDIMENT ALGORITHMS

A requirement fundamental to the validation of CZCS for the Great Lakes is the development of a working algorithm which can transform the satellite measured radiances into surface concentrations of chlorophyll and suspended sediment. While the ERIM task defined for current study involves development of water algorithms, these algorithms cannot in our estimation be attempted without some examination of and experimentation with atmospheric components. Thus, while we were able to place emphasis on certain water aspects of algorithm development, our approach has considered radiative transfer in the atmosphere. Our efforts to date have involved extensive use of statistical and model simulation techniques. Attempts to test candidate algorithms on real CZCS data have been limited because very few scenes of the Great Lakes were available and no CZCS tapes which correspond to the 1980 summer experiments are expected until mid 1981.

### 3.1 APPLICABILITY OF EXISTING ALGORITHMS

The removal of atmospheric effects is a necessary prerequisite for all remote sensing applications. Atmospheric effects are especially important in CZCS data for the following reasons.

1. The large swath width of the CZCS implies a large atmospheric variability due to simple considerations of scale as well as scan angle variations.
2. The inherent radiance of the water is low causing path radiance effects to be relatively more important than over land.
3. The CZCS includes wavelengths in the blue region of the spectrum where atmospheric effects predominate.

The study of atmospheric effects in CZCS data can be broken down into two levels. First, one can attempt to develop and/or validate radiative transfer models by making careful measurements of the relevant atmospheric parameters and of the radiance at the surface, and comparing the radiance measured by the satellite with that calculated from the model. Studies of this kind have been carried out for aircraft data at various altitudes [10] and for CZCS data over the Gulf of Mexico [11]. Aircraft studies have resulted in fairly good agreement between model predictions and measurements, although there is a discrepancy at large angles which is thought to be due to surface reflected skylight [10]. Previous studies with CZCS data have encountered some difficulty in obtaining agreement between model predictions and measurements [11]. One possible explanation for this difficulty is the effect of scattering from adjacent land areas which some studies have indicated to be of the same order of magnitude as the directly scattered path radiance [12]. In its studies ERIM will test existing models with aircraft measurements made during last summer's GLET experiments and with data obtained in the Gulf of Mexico Experiment [11].

A second kind of atmospheric study involves the development of operational algorithms for removing atmospheric effects from CZCS data without the use of an unreasonable number of in situ atmospheric measurements. The primary goal of these studies is to remove the variable component of the atmospheric effect using some property of the data itself to obtain the necessary correction parameters. One such algorithm was developed by Gordon [7] and applied to CZCS data over the Gulf of Mexico [10]. However, the formulation of Gordon's algorithm involves the assumption of zero intrinsic radiance in the 679 nm band which is not met in some parts of the Great Lakes and other coastal areas. Modifications to this algorithm have been made by a group at Scripps Institution of Oceanography for conditions occurring in Pacific coastal waters, but there is some doubt that their assumptions would hold in the Great Lakes. In addition to testing these algorithms, new directions have been pursued in the development of more suitable approaches.

## 3.2 OPTICAL MODELS AND RADIATIVE TRANSFER THEORY

Most existing algorithms are based upon empirical relationships between constituent concentrations and remotely sensed radiances, and are generally valid for the limited range of environmental conditions under which these relationships were derived. In order to systematically approach the evaluation of existing algorithms or the development of new algorithms, it is necessary to understand the relationships among the observed quantities on a more fundamental level. The study of these relationships is conveniently divided into two phases. The first phase deals with the inherent optical properties of the water and atmospheric constituents, and the second phase deals with the large-scale radiative transfer processes which relate these inherent optical properties to the radiances measured by the satellite.

### 3.2.1 OPTICAL MODELS

A full description of the optical properties of a passive (non-emitting) medium include the absorption coefficient and the volume scattering function. For most remote sensing purposes, however, it is not necessary to specify the complete volume scattering function. Commonly two parameters describing the scattering properties are considered: the total scattering coefficient (which is the integral of the volume scattering function over all angles), and the back-scattering coefficient (which is the integral of the volume scattering function over the angular range of  $90^\circ$  to  $180^\circ$  from the incident direction).

It is generally assumed that the inherent optical properties are linear functions of the concentrations of the various constituents of the medium. Thus, for natural bodies of water we can write



$$\begin{aligned}
 a &= a_w + \sum_{i=1}^N \hat{a}_i C_i \\
 Bb &= Bb_w + \sum_{i=1}^N \hat{Bb}_i C_i \\
 b &= b_w + \sum_{i=1}^N \hat{b}_i C_i
 \end{aligned}
 \tag{1}$$

where  $a_w$ ,  $Bb_w$ , and  $b_w$  are the absorption, backscattering, and total scattering coefficients of pure water;  $\hat{a}_i$ ,  $\hat{Bb}_i$ , and  $\hat{b}_i$  are the absorption, backscattering, and total scattering cross sections (i.e., the coefficients for unit concentration) of constituent  $i$ , and  $C_i$  is the concentration of constituent  $i$ . These are clearly approximations, since the actual optical properties may depend upon factors other than the concentrations. The scattering properties of suspended particulates, for example, depends upon the size distribution as well as the mass per unit volume. Some preliminary studies of the effect of size distribution are described in section 3.3.

Accepting the linear model for the optical properties described above, there are several possible approaches to the determination of the absorption and scattering cross sections for each constituent. One approach would be to attempt to isolate each constituent and measure the optical properties for different concentrations of that constituent. Isolation can obviously be accomplished more easily with some types of constituents than with others. The danger of this approach is that by artificially changing the sample, the measured conditions might not be representative of naturally occurring waters.

A second approach for determining the optical cross sections is to measure the optical properties and the constituent concentrations of a large number of diverse natural samples, and performing a statistical analysis (i.e., a multiple linear regression) of the results. This approach avoids the possibility of encountering unrealistic conditions, but is subject to biases introduced by natural correlations between various constituents, for example between phytoplankton and sediments

associated with phytoplankton nutrients. Examples of this approach include the work of Bukata et al [13] and the preliminary analysis presented in section 3.3 of this report.

It should be pointed out that some of the optical properties, i.e., the scattering cross sections, can be calculated from electromagnetic theory if the size distribution, shapes, and indices of refraction of the particles are known. Although it is instructive to make such calculations in order to determine the sensitivity of the cross sections to the size distribution, for example, there is no particular advantage to the exclusive use of this method since it requires measurements which are at least as difficult as the direct measurement of the optical properties.

### 3.2.2 RADIATIVE TRANSFER THEORY

The radiance at any point in the ocean/atmospheric system is provided, in principle, by the solution of the radiative transfer equation with the proper boundary conditions and the proper optical properties specified at each point. Unfortunately, an exact solution of this equation is not obtainable in closed form for even the simplest geometry. Two general types of approach are, therefore, possible. The first approach is to develop approximate solutions which give reasonably accurate results over the range of conditions encountered. The advantage of this approach is that results can be obtained at a relatively low cost, and that considerable insight can be gained by merely examining the functional form of the solutions.

The alternative approach is to develop exact numerical solutions of the radiative transfer equation. Several types of numerical solutions exist, perhaps the most prominent for this application being the Matrix Operator and Monte Carlo methods. The Monte Carlo method is especially powerful because of its ability to incorporate complex boundary conditions (e.g., at the water surface) and spatially variable optical properties. The advantage of the numerical approach is, of course, the

accuracy of the results. The disadvantages are the cost of obtaining these results and the fact that insight can be gained into the nature of the solutions only by examining a large number of cases with different input parameters.

The preliminary modeling work done on this project has involved a combination of the approaches described above. For the purpose of formulating candidate algorithms it has been useful to consider a simplified model in which the water radiance is calculated using Gordon's Power Series Approximation, and the atmospheric effects are described by a model which assumes constant transmittance and a path radiance which is a linear function of the aerosol optical depth. According to this model, the radiance at the satellite is given by

$$L = L_p(\tau_a) + TE\rho_w(x) \quad (2)$$

where

$L_p(\tau_a)$  = path radiance (assumed to be a linear function of the aerosol optical depth  $\tau_a$ )

$T$  = atmospheric transmittance (assumed constant)

$E$  = irradiance at water surface (assumed constant)

$$\rho_w(x) = \frac{T_{w1} T_{w2} x}{2\pi n^2 (\mu + \mu_0)}$$

$$x = \frac{Bb}{a + Bb} \quad (\text{c.f. previous definitions of } a \text{ and } b \text{ in text})$$

$T_{w1}, T_{w2}$  = water surface transmittance for incoming and outgoing light

$\mu_0, \mu$  = cosine of solar zenith angle and observation angle, respectively

$n$  = index of refraction of water

The algorithms developed using this model are described in sections 3.4 of this report. For the purpose of evaluating these and other algorithms, a more comprehensive simulation model was also developed. This model incorporates the Monte Carlo calculations of the subsurface water reflectance using the following power series expansion [14]

$$\rho_w(x) = \frac{T_{w1} T_{w2}}{\pi n^2} [ .0001 + .3244x + .1425x^2 + .1308x^3 ]$$

where  $x$  is defined as previously. Atmospheric effects are calculated using the QSS model for the path radiance, and the double-delta model [11] for the irradiance and sky radiance. The surface-reflected sky radiance is included, assuming a nominal surface reflectance of 2.0 percent. The atmospheric state is described in terms of the horizontal visibility using the relationships developed by Elterman [15] to calculate the optical depth. The results of this simulation model are presented in section 3.5 of this report.

### 3.3 PRELIMINARY ANALYSIS OF OPTICAL PROPERTIES FOR THE GREAT LAKES

During late July 1980 twenty-one individual samples gathered by LeRC were analyzed by the NASA/Langley research Center (LaRC) portable laboratory stationed at the LeRC flight facility. Samples were flown in on the same day as collection and usually received by the LaRC staff within four hours for analysis. Underwater optical properties were measured in vitro with identical spectral range (400-800 nm) and intervals (50 nm). These properties included absorption, beam attenuation, and volume scattering. Three separate instruments were used to measure these parameters, (1) a combination beam attenuation and small angle scattering meter (SASM,  $\theta = 0.379, 0.751, 1.49^\circ$ ) developed by LaRC and patterned after the Scripps Institution of Oceanography ALSCAT instrument; (2) a Brice Phoenix (BP) scattering meter modified to accommodate large angle measurements ( $25^\circ \leq \theta \leq 155^\circ$ ); and (3) the LaRC spectral absorption coefficient instrument (SPACI) [16]. Standard errors for these

instruments are reported to be as follows: (1) for the SASM less than 5%  $\alpha$ , and less than 12%  $\beta(\theta)$ ; and (3) for the SPACI less than 10%  $a$ .

The optical measurements made by LaRC during the 1980 summer experiments were for lake samples. In this case the measured optical properties pertain to the particular mix of constituents in the lake sample. If sufficient number of measurements are made in this manner and if the principal constituents present are known then multiple regression techniques can be used to derive the optical cross sections for a common constituent. While the present data are considered limited for this purpose a preliminary set of optical properties were derived for the Great Lakes.

Of the twenty-one optical data sets taken, three Lake Erie samples contained sufficient quantities of sediment to saturate the optical measurement instruments. Samples collected from Green Bay in Lake Michigan and from Western Lake Superior were found to have distinctive local optical properties. Four of the six samples collected from the Grand Haven area were essentially sediment-free and the presence of very low concentrations of phytoplankton made absorption measurements difficult. Attempts to include these samples in the regression analysis have so far not been productive.

The best regression results were obtained when nine samples from Lake Erie were combined with two samples from Lake Michigan. Several regression models were formulated and tested against the above selected optical measurement sets. These models were based upon the available surface truth sampling data which included Secchi depth, surface temperature, chlorophyll-a pigment, phaeophytins, and residue (total, ashed, and volatile) [17]. Of these parameters chlorophyll-a, chlorophyll-a plus phaeophytins, total residue and ashed residue were selected for regression. Each of the candidate models contained two components and a constant which includes absorption or scattering for pure water. Models involving ashed residue produced generally better statistics than

those with total residue. Each regression model consists of four equations pertaining to the backscatter cross section. In each case the four equations correspond to four CZCS wavelengths (443, 520, 550, 670 nm). The optical model considered for these analyses describes the surface water mass to be a combination of pure water (w), unique organics as represented by chlorophyll-a (chl) and phaeophytin (pp) concentration and unique inorganics as represented by the measurement of suspended minerals (sm). The two component model equations are written as

$$a(\lambda) = a_w(\lambda) + xa_{chl}(\lambda) + ya_{sm}(\lambda) + \text{constant } a(\lambda)$$

$$Bb(\lambda) = Bb_w(\lambda) + xBb_{CHL}(\lambda) + yBb_{sm}(\lambda) + \text{constant } Bb(\lambda)$$

where x and y are the concentrations of chlorophyll a and suspended minerals (ashed weight) respectively, and a and Bb are the absorption and backscatter cross sections.

Optical cross sections as derived from these regression analyses are given in Table 2. These optical cross sections are the only such data available, to our knowledge for the Great Lakes. Note that the  $a_w$  or  $Bb_w$  are included in the constant term given for each analysis. As shown in Table 2, two preliminary optical models were derived based upon chlorophyll-a and chlorophyll + phaeophytin concentrations, respectively. Also shown for comparison are values of four and five component Lake Ontario models [18] which were derived indirectly from apparent rather than inherent optical measurements. The four component model included chlorophyll, suspended sediment, pure water, and dissolved organics. The five component model has an additional term for non living organics which includes detritus. The dissolved organics term accounts for the presence of yellow substance which was found in the Ontario study to be about 2 mg/l and fairly constant throughout the

TABLE 2

## OPTICAL CROSS SECTIONS FOR GREAT LAKES WATER QUALITY MODELS

## (1) Great Lakes 1980 Preliminary Models

Model 1a	Wavelength (nm)	$a_{\text{CHL}}$ ( $\text{m}^2/\text{mg}$ )	$a_{\text{sm}}$ ( $\text{m}^2/\text{g}$ )	Constants	Multiple Regression Coefficient
	443	.01620	.0764	.3088	.961
	520	.00836	.0636	.2484	.952
	550	.00529	.0577	.3034	.945
	670	.00450	.0556	.3897	.942
		$Bb_{\text{CHL}}$ ( $\text{m}^2/\text{mg}$ )	$Bb_{\text{sm}}$ ( $\text{m}^2/\text{g}$ )		
	443	.000152	.0312	.0424	.900
	520	.000372	.0284	.0370	.911
	550	.000469	.0287	.0232	.911
	670	.000428	.0250	.0197	.913
Model 1b		$a_{\text{CHL+pp}}$ ( $\text{m}^2/\text{mg}$ )	$a_{\text{sm}}$ ( $\text{m}^2/\text{g}$ )		
	443	.01142	.07290	.3794	.970
	520	.00599	.06178	.2813	.963
	550	.00384	.05658	.3220	.954
	670	.00323	.05468	.4072	.947
		$Bb_{\text{CHL+pp}}$ ( $\text{m}^2/\text{mg}$ )	$a_{\text{sm}}$ ( $\text{m}^2/\text{g}$ )		
	443	.000043	.03117	.04590	.890
	520	.000213	.02832	.0408	.910
	550	.000273	.02856	.0277	.910
	670	.000254	.02490	.0237	.912

## (2) Lake Ontario Five Component Model

	$a_{\text{CHL}}$ ( $\text{m}^2/\text{mg}$ )	$a_{\text{sm}}$ ( $\text{m}^2/\text{g}$ )	Constant
443	.0354	.0557	.020
520	.0240	.0281	.028
550	.0173	.0185	.037
670	.0100	.0225	.370

	$Bb_{CHL} (m^2/mg)$	$Bb_{sm} (m^2/g)$	Constant
443	.00199	.0328	0
520	.00182	.0474	0
550	.00241	.0525	0
670	.00175	.0333	0

(3) Lake Ontario Four Component Model

	$a_{CHL} (m^2/mg)$	$a_{sm} (m^2/g)$	Constant
443	.0343	.0557	.185
520	.0232	.0281	.119
550	.0173	.0185	.122
670	.0105	.0225	.388

	$Bb_{CHL} (m^2/mg)$	$Bb_{sm} (m^2/g)$	Constant
443	.00163	.0328	.0010
520	.00153	.0474	-.0058
550	.00202	.0525	-.0099
670	.00156	.0333	-.0080



lake. Since for the present study no effort was made to analyze the samples for a non-living organics or dissolved organics term they were not included in our preliminary model except as part of the constant term.

The absorption cross sections as derived from the 1980 optical measurement sets are for chlorophyll, about half of those derived for the Lake Ontario models. Derived chlorophyll backscatter coefficients were found to be only one tenth of those obtained by the Lake Ontario study. Chlorophyll absorption and scattering cross sections as obtained by regression are considerably less than those reported elsewhere in the literature [17]. On the other hand, derived optical cross sections for the suspended sediment are comparable to the Lake Ontario values.

All of the above models have utilized phaeophytin free chlorophyll determinations. Since chlorophyll and phaeophytins have similar absorption properties they cannot be readily distinguished by CZCS. Therefore, it seemed appropriate to combine these determinations in the above regression analyses and determine cross sections for chlorophyll plus phaeophytin. The resulting cross sections as given in Table 2 model 1b are smaller for the chlorophyll term and larger for the constant term than in the phaeophytin free analysis of model 1a. Since the direction of these changes are opposite to our expectations, additional investigation into the optical properties of phaeophytins is warranted.

In addition to the statistical analyses of the collected samples described above a brief investigation was made of an indirect technique for measuring scattering and absorption properties of suspended sediment in Lake Erie. The approach involved making a series of physical and optical measurements on a single turbid water sample at various time intervals. A portion of the suspended sediment was allowed to settle out between each measurement. Optical parameters measured by the LaRC portable laboratory included the beam attenuation coefficient and the volume scattering function at  $90^\circ$ . Both of these measurements were made

at a single wavelength of 550 nm. Physical measurements included the particle size distribution (using a Coulter counter) and the total suspended solids concentration. There were two objectives to these measurements. First the change in suspended solids concentration could be related to the corresponding change in the optical properties from which optical cross sections could be obtained. Second, Mie particle scattering theory could be used to calculate the same optical properties based upon the change in particle size distribution. Unfortunately, the total suspended solids measurements were found to be unreliable, either because of sampling or measurement errors, and were not included in the analysis. The optical measurements are summarized in Table 3, and the particle size measurements are shown in Figure 2 (panel a). It should be noted that Coulter counter measurements are difficult and subject to considerable error in the particle size range necessary for studies of this kind.

Because of the unreliability of the total suspended solids measurements, it was not possible to derive the optical cross sections directly from this set of measurements. Instead, the data set was used to test the feasibility of the approach of calculating the optical properties with Mie scattering theory. Of course, these calculations also requires a knowledge of the index of refraction of the particles. Since no measurements of the index of refraction were made, an average value of 1.1 was assumed. The extinction efficiency was calculated from the Mie theory using J.V. Dave's algorithm [19] for particle diameters between 1.0 and 25.4  $\mu\text{m}$ . The portion of the total extinction coefficient arising from this particle size range was then obtained for each sample by multiplying by the size distribution function and integrating (summing) over this range. For particle diameters less than 1 micron, the extinction efficiency was calculated using Van de Hulst's approximation [20].

$$Q_{\text{ext}} = 2 - \frac{4}{\rho} \sin \rho + \frac{4}{\rho^2} (1 - \cos \rho) \quad (6)$$

TABLE 3  
OPTICAL MEASUREMENTS MADE DURING SETTLING EXPERIMENT

Sample	Settling Time (hrs)	$\alpha(550 \text{ nm})$	$\beta(90^\circ, 550 \text{ nm})$
1	0	$23.7 \text{ m}^{-1}$	$0.1380 \text{ m}^{-1} \text{ sr}^{-1}$
2	1.5	$19.3 \text{ m}^{-1}$	---
3	19.0	$8.7 \text{ m}^{-1}$	$0.0685 \text{ m}^{-1} \text{ sr}^{-1}$
4	23.5	$7.0 \text{ m}^{-1}$	$0.0617 \text{ m}^{-1} \text{ sr}^{-1}$
5	40.0	$4.5 \text{ m}^{-1}$	$0.0319 \text{ m}^{-1} \text{ sr}^{-1}$

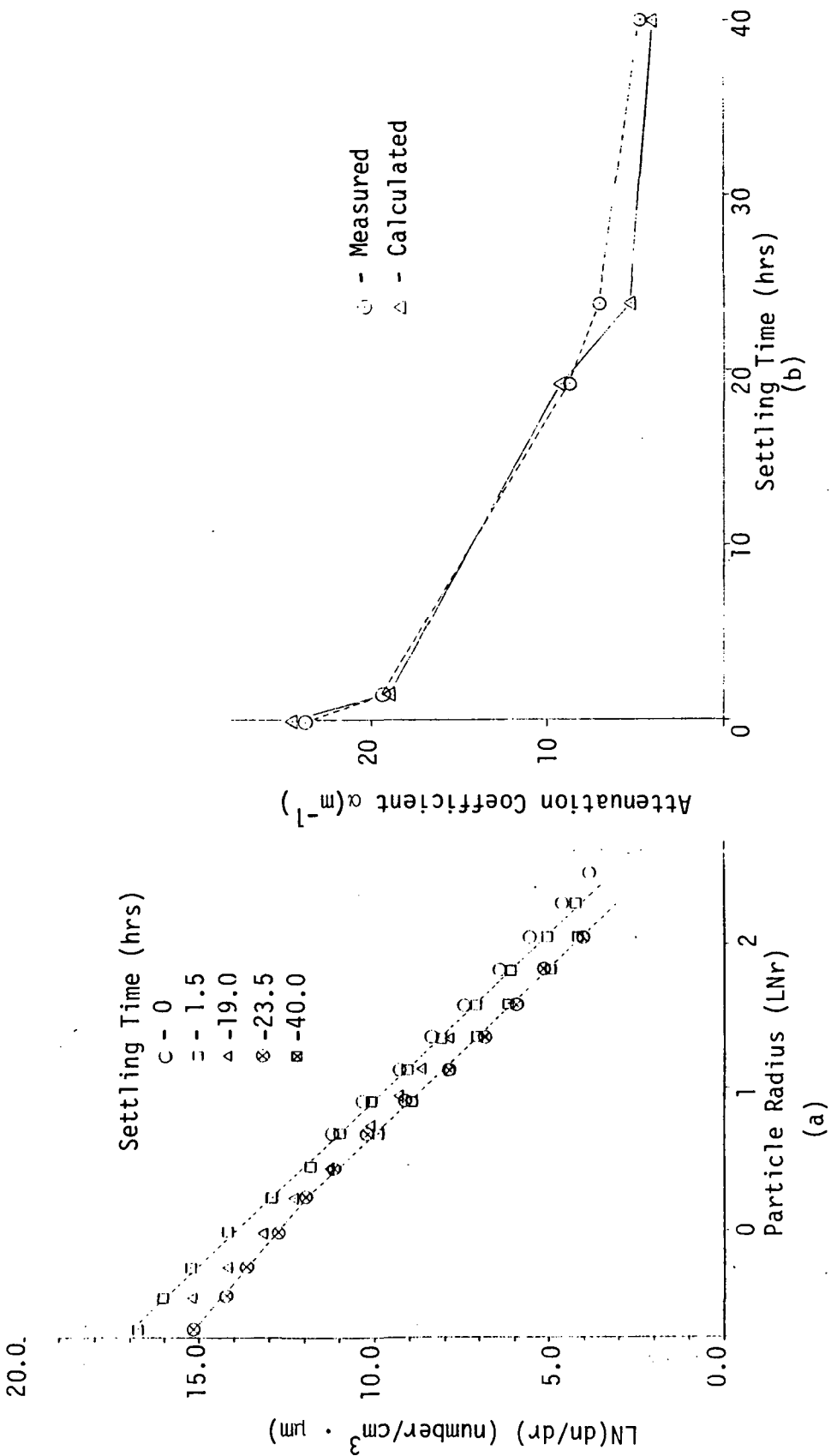


FIGURE 2. RESULTS FROM THE LAKE ERIE SETTLING EXPERIMENT. Panel (a) shows the particle size distribution measured at selected time intervals. Panel (b) compares measured attenuation coefficient with that calculated from the particle size distribution based upon Mie scattering theory.

where

$$\rho = \frac{4\pi(n-1)r}{\lambda}$$

( $n$  is the index of refraction and  $\lambda$  is the wavelength). The contribution to the total extinction coefficient from particles less than 1 micron in diameter is then given by

$$\sigma'_{\text{ext}} = \int \pi r^2 Q_{\text{ext}} \left( \frac{dn}{dr} \right) dr \quad (7)$$

For this particle size range, the size distribution was assumed to have the form

$$\frac{dn}{dr} = cr^{-4} \quad (8)$$

where  $c$  is chosen to fit the measurement of  $r = 0.5 \mu\text{m}$ . The extinction coefficients calculated from this procedure are shown in Table 4, and are compared with the measured extinction coefficients in Figure 2 (panel b). In view of all the uncertainties and assumption required to make these calculations the agreement shown is surprisingly good. While these results are obviously insufficient to validate the approach they do suggest that further controlled studies of this type would be beneficial. If a technique could be derived for universal Coulter Counter measurements instead of the present elaborate and not readily available optical measurements the overall benefits of the present program would be substantial.

### 3.4 DISCUSSION OF ATMOSPHERIC EFFECTS AND CORRECTIONS

A necessary preliminary step before attempting to extract any information about the water itself is to remove the effects of atmospheric variations from the measured radiances. Atmospheric effects are

TABLE 4

## EXTINCTION COEFFICIENTS CALCULATED FROM MIE SCATTERING THEORY

Sample	Contribution From $r < 0.5 \mu\text{m}$	Contribution From $r > 0.5 \mu\text{m}$	Total ext ( $\text{m}^{-1}$ )
1	7.2	18.3	25.5
2	4.8	14.1	18.9
3	2.5	6.7	9.2
4	1.0	4.3	5.3
5	0.7	3.2	3.9

particularly important in CZCS data because of the large swath width and the band placement. The development of radiative transfer models for the atmosphere is an important step in understanding this problem, but ultimately the goal must be to remove the atmospheric effects on a point-by-point basis with the aid of only a very limited number of external measurements.

The first attempt to formulate such an atmospheric correction algorithm for CZCS data was made by Gordon [7]. This algorithm is based upon the assumption that the total radiance in a suitable wavelength band may be interpreted as an index of the atmospheric state (i.e., the aerosol optical depth) and thus used to correct the atmospheric effects in the other bands. In this formulation it is assumed that the water radiance in the 670 nm band is zero or negligible compared to the path radiance, an assumption which is valid in clear ocean waters but is frequently violated in more turbid coastal waters, including the Great Lakes. In fact, our modeling study has shown the 670 nm band displays the greatest sensitivity to sediment concentration. Therefore, although the algorithm gives apparently good results in ocean areas [1] it cannot be applied directly to the Great Lakes.

The assumptions about the atmosphere in Gordon's algorithm seem to be valid for a reasonably wide range of atmospheric variations. These assumptions are essentially the same as those listed for the simplified model described in section 3.2, namely: (1) the path radiances in the various wavelength bands are linearly related to each other, and (2) the atmospheric transmittance changes relatively slowly and may be assumed constant. Under these assumptions one can define a large class of linear combinations.

$$X_i = \sum_{j=1}^N A_{ij}L_j \quad (9)$$

which are independent of atmospheric variations. Gordon's algorithm is one member of this class, but is not necessarily the optimum one. The condition for the  $X_i$ 's to be independent of atmospheric variations can be written as

$$\sum_{j=1}^N A_{ij} \frac{\partial L_{pj}}{\partial \tau_a} = \sum_{j=1}^N A_{ij} A_j' = 0 \quad (10)$$

where  $i=1\dots N-1$ ,  $L_{pj}$  is the path radiance in band  $j$  and  $\tau_a$  is the aerosol optical depth. The coefficients  $A_{ij}$  may be interpreted as components of the vector  $\vec{A}_i$ , and the above condition viewed as the requirement that these vectors be perpendicular to the vector

$$A_N = (A_1', A_2', \dots, A_N') \quad (11)$$

If we require in addition that the vectors  $\vec{A}_1 \dots \vec{A}_{N-1}$  be orthonormal, i.e.,

$$\vec{A}_i \cdot \vec{A}_j = \begin{cases} 0, & i \neq j \\ 1, & i = j \end{cases} \quad (12)$$

then the transformation (9) has the properties of a projection onto a hyperplane perpendicular to  $\vec{A}_N$ , and the projected variables are linearly independent of each other. Although this would seem to be a desirable condition, the actual benefits of this procedure, as opposed to Gordon's procedure for example (which does not satisfy equation (12)), have not yet been demonstrated. Work has begun on the evaluation of this procedure using the simulation model described in section 3.2, but a full comparison with Gordon's algorithm has not yet been completed.

It should be noted that the direction of the vector  $A_N$  can be determined empirically from the CZCS data itself, if an area of variable haze over a uniform water background can be located in the image. The



direction cosines are obtained readily by a principal components analysis of the radiances observed over such an area.

As discussed previously in section 3.2 the signal variants due to spatial changes in the aerosol content (haze) are linear. As discussed by Gordon in his correction method the aerosol contribution at one wavelength is approximately proportional to the other wavelengths. In CZCS four channel signal space, atmospheric variation is visualized as a vector oriented by these proportions and offset from the origin by the presence of water constituents and atmospheric transmittance effects. By comparison the water variants represent separate orientations for each constituent and generally much smaller than the atmospheric haze vector. Thus for open clear waters of the Great Lakes the observed variations are due essentially to atmospheric haze and system noise.

In order to explore the haze phenomenon several segments from two available CZCS images were examined. Each segment (200-1000 pixels) was first scaled to radiance and then analyzed for principal components. Two available CZCS scenes were selected for analysis: Great Lakes May 8, 1979 and Gulf of Mexico, November 9, 1978. Results of these analyses are shown in Table 5. Also shown is the principal component for atmospheric variation as derived from simulations using the preliminary atmospheric model discussed in section 3.2. Atmospheric vectors derived by this analysis show strong similarity in orientation. Differences in orientation are likely due to cloud effects and variations in water constituents. Radiometric changes due to scan angle effect may also account for some of the observed differences. Excellent agreement ( $1.1^\circ$ ) was found between the combination of Lake Huron data sets and the theoretical orientation of the haze vector. In general, the orientation of the haze vector for the Gulf of Mexico data sets were similar to those for Lake Huron but with less consistency and lower accounting of the percent of total variance. Clouds and variation of chlorophyll and suspended materials could possibly account for the observed variability in principal components.

TABLE 5  
FIRST PRINCIPAL COMPONENTS DERIVED FROM  
CZCS SATELLITE MEASURED RADIANCES

Sample Location	First Principal Component	Percent of Total Variance
Georgian Bay, Lake Huron (1)	(.563, .539, .543, .313)	94.8%
Georgian Bay, Lake Huron (2)	(.440, .499, .565, .488)	94.2
Southern Lake Huron	(.435, .577, .594, .355)	95.4
Combination Set, Lake Huron	(.426, .5520, .547, .500)	95.5
Gulf of Mexico (2)	(.596, .580, .467, .298)	98.3
Gulf of Mexico (3)	(.487, .548, .538, .416)	94.8
Gulf of Mexico (4)	(.559, .597, .465, .339)	91.7
Gulf of Mexico (5)	(.604, .679, .330, .256)	85.1
Combination Set, Gulf of Mexico	(.521, .579, .518, .353)	87.4
Atmospheric Model	(.426, .510, .524, .533)	100.0

CZCS Imagery

Lake Huron: May 8, 1979 Orbit 2715

Gulf of Mexico: November 9, 1978 Orbit 227

An analysis was made to observe if the haze vector was present and significant in apparent low haze area. Several samples were selected in the May 8 image from a test area south of Nova Scotia in the open ocean and at least 160 kilometers from the US mainland. The image appeared to be free of haze. Nevertheless the haze vector appeared as the principal component in each sample and subsample and with as few as fifteen pixels. These analyses further demonstrate the need to account for the atmospheric variants even under the clearest of conditions.

### 3.5 PRELIMINARY CZCS WATER ALGORITHMS

The atmospheric, interface, and subsurface water reflectance models discussed in section 3.2 were used to calculate expected satellite radiances for a variety of water masses at each of the CZCS wavelengths. The primary input for these calculations were the optical cross section data as described per the three optical models in section 3.3. Different water masses were simulated by varying the concentrations of chlorophyll and suspended mineral concentrations. In the case of the Lake Ontario five component model the level of non-living detrital material was taken as 2.0 mg/l and dissolved organics at 2.5 mg/l. These levels are similar to those measured in the Lake Ontario study [13]. Presently we have no measurement data to support the representativeness of these values to Lakes Erie or Michigan.

Having made these assumptions the subsurface irradiance reflectance can be readily calculated for each CZCS band (443, 520, 550, 670 nm) as a function of the concentration of chlorophyll and suspended minerals. The spectral characteristics of the irradiance reflectance function can be depicted with iso-concentration curves for each pair of wavelengths. Figures 3, 4, and 5 show calculated subsurface reflectance for each of the two Lake Ontario models and the preliminary 1980 optical model, respectively. Each of the four panels of each figure has nine curves of increasing suspended mineral concentration and constant value of chlorophyll pigment concentration (0.0, 1.0, 2.0, 5.0, 10.0, 20.0, 50.0,

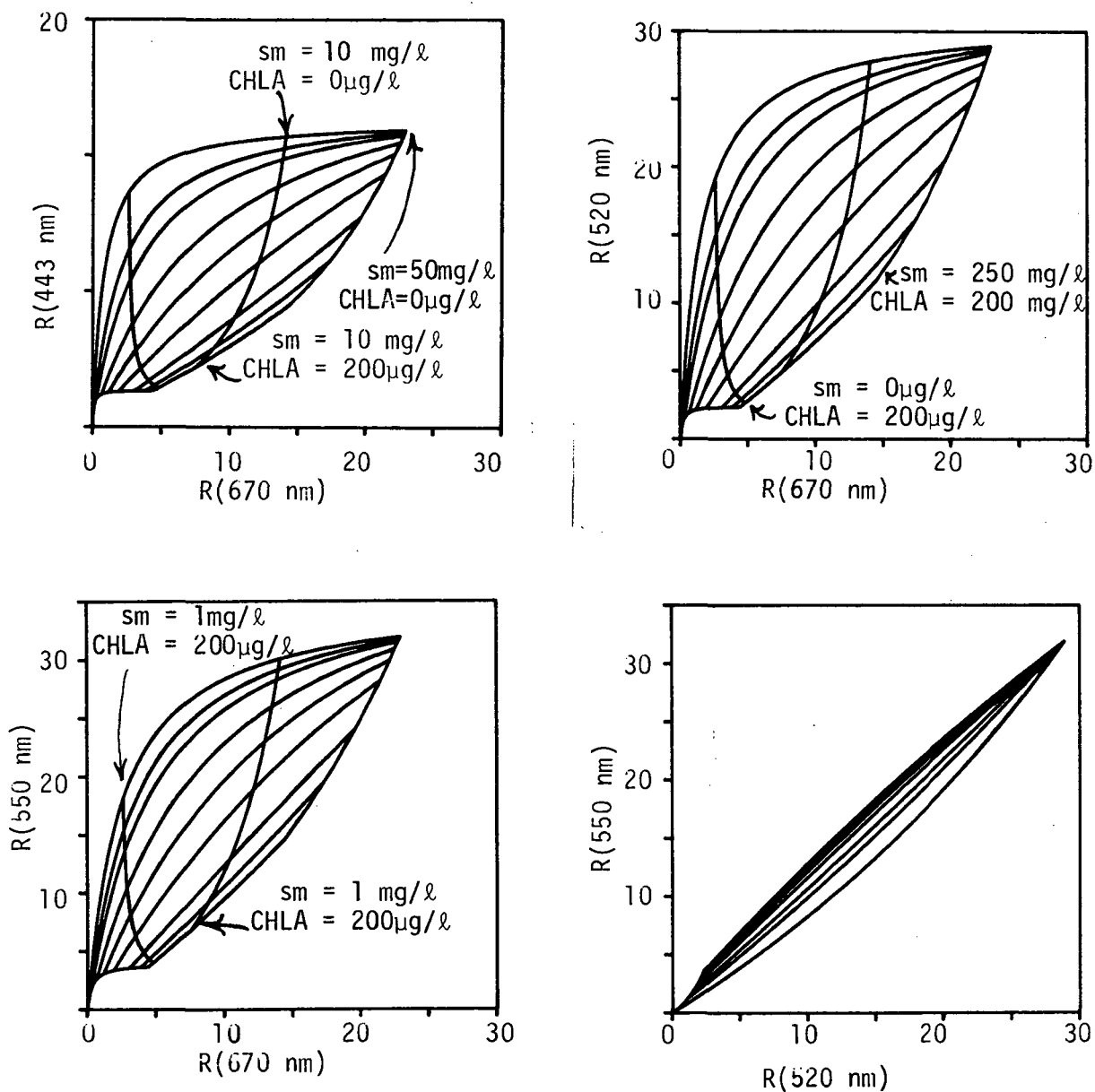


Figure 3. Subsurface reflectance (percent) at CZCS wavelengths (443 nm, 520 nm, 550 nm, 670 nm) as predicted by the Lake Ontario 5-component model [18]. Each figure has nine parametric curves of increasing suspended mineral concentration (0.0-50.0 mg/l) with constant values of chlorophyll pigment concentration (0.0, 1.0, 2.0, 5.0, 10.0, 20.0, 50.0, 100, 200  $\mu\text{g}/\ell$ ). Each figure also contains four parametric curves of increasing chlorophyll a (0.0-200.0  $\mu\text{g}/\ell$ ) at constant values of suspended mineral concentration (0.0, 1.0, 10.0, 50.0 mg/l).

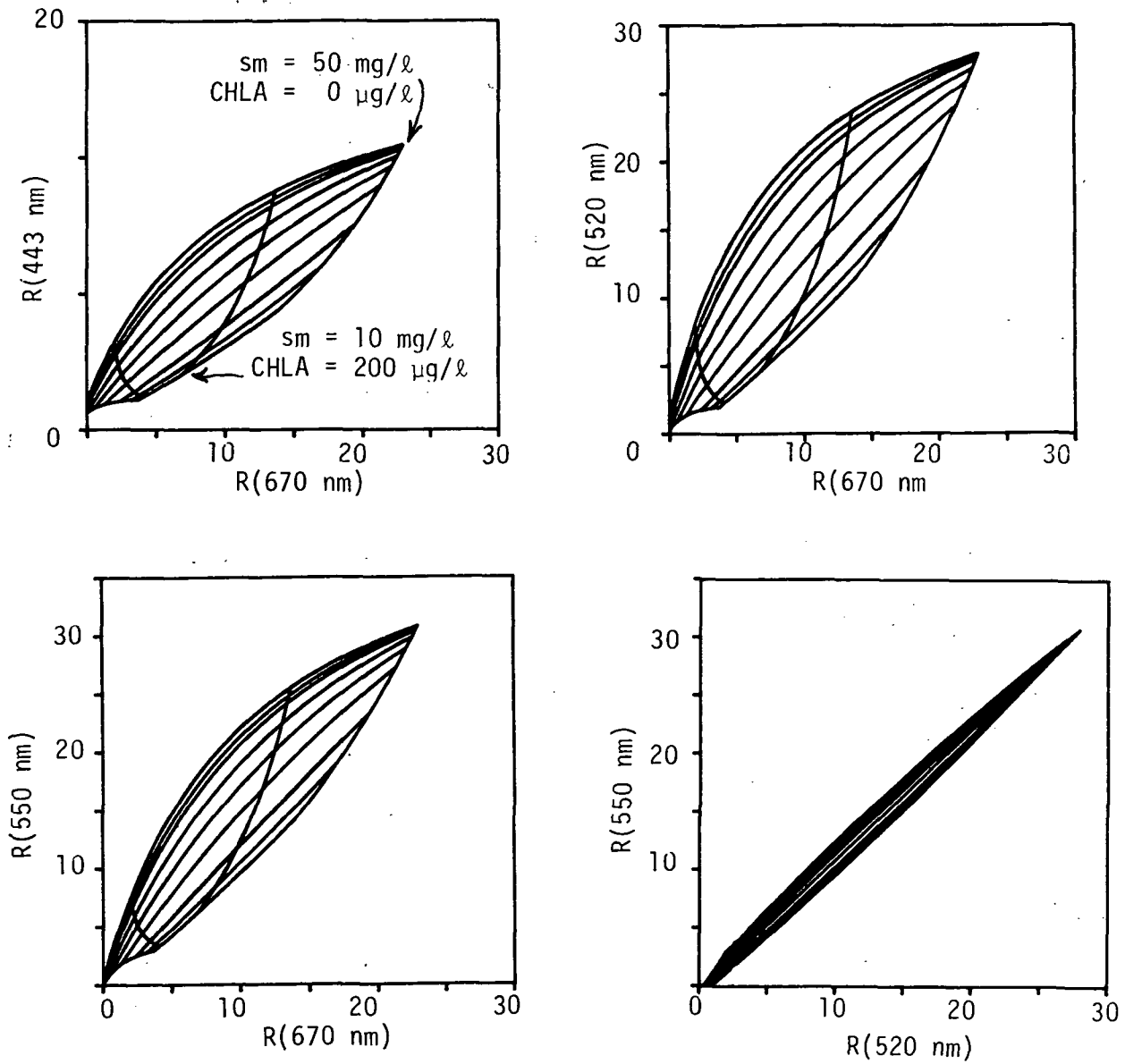


Figure 4. Subsurface reflectance (percent) at CZCS wavelengths (443 nm, 520 nm, 550 nm, 670 nm) as predicted by the Lake Ontario 4-component model [18]. Each figure has nine parametric curves of increasing suspended mineral concentration (0.0-50.0 mg/l) with constant values of chlorophyll pigment concentration (0.0, 1.0, 2.0, 5.0, 10.0, 20.0, 50.0, 100, 200 µg/l). Each figure also contains four parametric curves of increasing chlorophyll a (0.0-200.0 µg/l) at constant values of suspended mineral concentration (0.0, 1.0, 10.0, 50.0 mg/l).

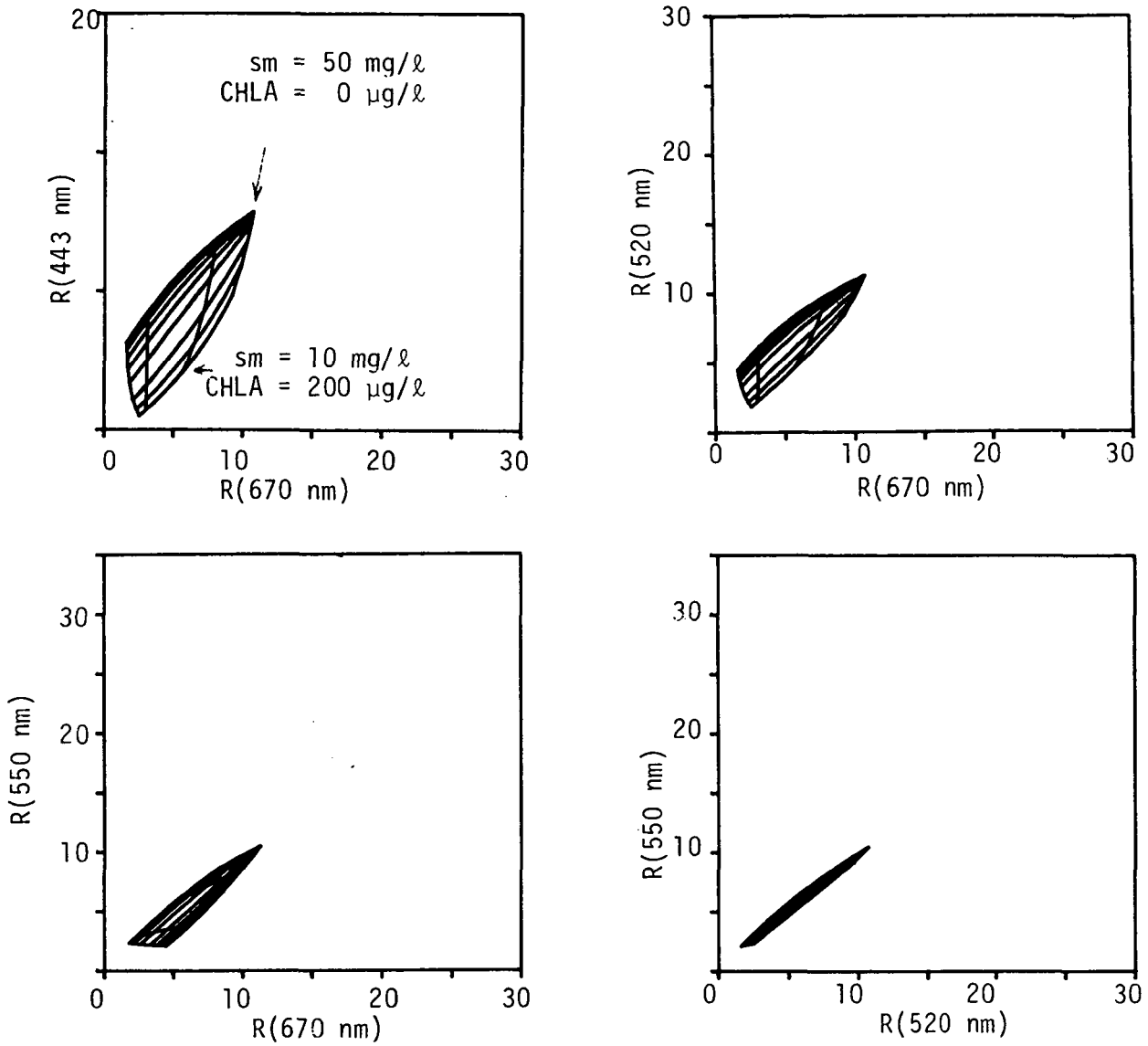


Figure 5. Subsurface reflectance (percent) at CZCS wavelengths (443 nm, 520 nm, 550 nm, 670 nm) as predicted by the Preliminary 1980 Optical Model. Each figure has nine parametric curves of increasing suspended mineral concentration (0.0-50.0 mg/l) with constant values of chlorophyll pigment concentration (0.0, 1.0, 2.0, 5.0, 10.0, 20.0, 50.0, 100, 200  $\mu\text{g/l}$ ). Each figure also contains four parametric curves of increasing chlorophyll a (0.0-200.0  $\mu\text{g/l}$ ) at constant values of suspended mineral concentration (0.0, 1.0, 10.0, 50.0 mg/l).

100, and 200  $\mu\text{g}/\ell$ ). These curves tend to converge to a point beyond the calculated range. One could refer to this ideal point as the "point of all sediment". Each figure also contains four curves of increasing chlorophyll with constant values of sediment (0.0, 1.0, 10.0, and 50.0  $\text{mg}/\ell$ ). These latter iso-concentration curves tend to converge in several of the panels to a point on the 670 nm axis. This ideal could be referred to as the "point of all chlorophyll". Each panel of these figures is a projection and together suggest the reflectance space is a three dimensional hyperplane and nearly perpendicular to the  $R(550)/R(520)$  plane.

For the five component Lake Ontario model the constant optical cross sections are very small relative to those for chlorophyll and sediment. As a result the sensitivity of reflectance to changes in concentration is large. By comparison the Lake Ontario four component model has slightly smaller cross sections and a larger constant term. Consequently the panel figures are slightly smaller. The effect of the relatively small optical cross sections of the preliminary 1980 optical model with a large constant term is shown by the small magnitudes of change in each panel of Figure 5. The difficulties of using this latter optical model to predict concentrations is apparent. The above figures also show generally that reflectance is more sensitive to changes in sediment (as  $\text{mg}/\ell$ ) than chlorophyll (as  $\mu\text{g}/\ell$ ) which is consistent with their relative optical cross sections.

As discussed in the previous section, the spectral changes observed in CZCS data due to chlorophyll and sediment will be influenced by the presence of atmospheric variants. A principal component analysis of pure chlorophyll and sediment data indicated spectral orientation with angular separations from the pure atmospheric vector of  $26.1^\circ$  and  $18.7^\circ$ , respectively. Thus it seems apparent that the atmospheric variants are indeed coupled to those we wish to determine in the water. Unless there is some way to separate the atmospheric and water components by spatial filtering it seems appropriate to remove this influence by projecting

these reflectance data along the atmospheric vector. This projection reduces the four dimensional reflectance space to one of three dimensions which is free of any atmospheric influence. Figure 6 shows the projected space for each of the three optical models under consideration. The panel figures on the right are nearly a planer view of the depicted leaf like projected structure. Thus corresponding projected axis hold promise for deciphering the water components. Since there are an infinite set of transformations which will project the four dimensional reflectance space into three dimensions the panel figures shown can be rotated to any orientation. This feature may provide a means to later optimize candidate algorithms.

Thus far our efforts to obtain chlorophyll and sediment algorithms have utilized the above projection technique. Using non-linear regression techniques algorithm prediction equations were derived as third order, second degree polynomials with nine terms. These equations have the following form:

$$f(\text{conc}) = C_1(R_1')^2 + C_2(R_2')^2 + C_3(R_3')^2 + C_4(R_1', R_2') + C_5(R_1', R_3') + C_6(R_2', R_3') + C_7 R_1' + C_8 R_2' + C_9 R_3' + C_{10} \quad (13)$$

where the R's refer to the three axis of projection and the C's are the multiple regression coefficients.

Using the model described in section 3.2 and the optical properties of Table 2 data sets of simulated CZCS radiances were generated for water quality conditions similar to those that exist in the Great Lakes. Several simulation data sets were generated for each model. These included each of the following types:

- (1) Variable chlorophyll, fixed sediment, fixed haze, zero system noise;



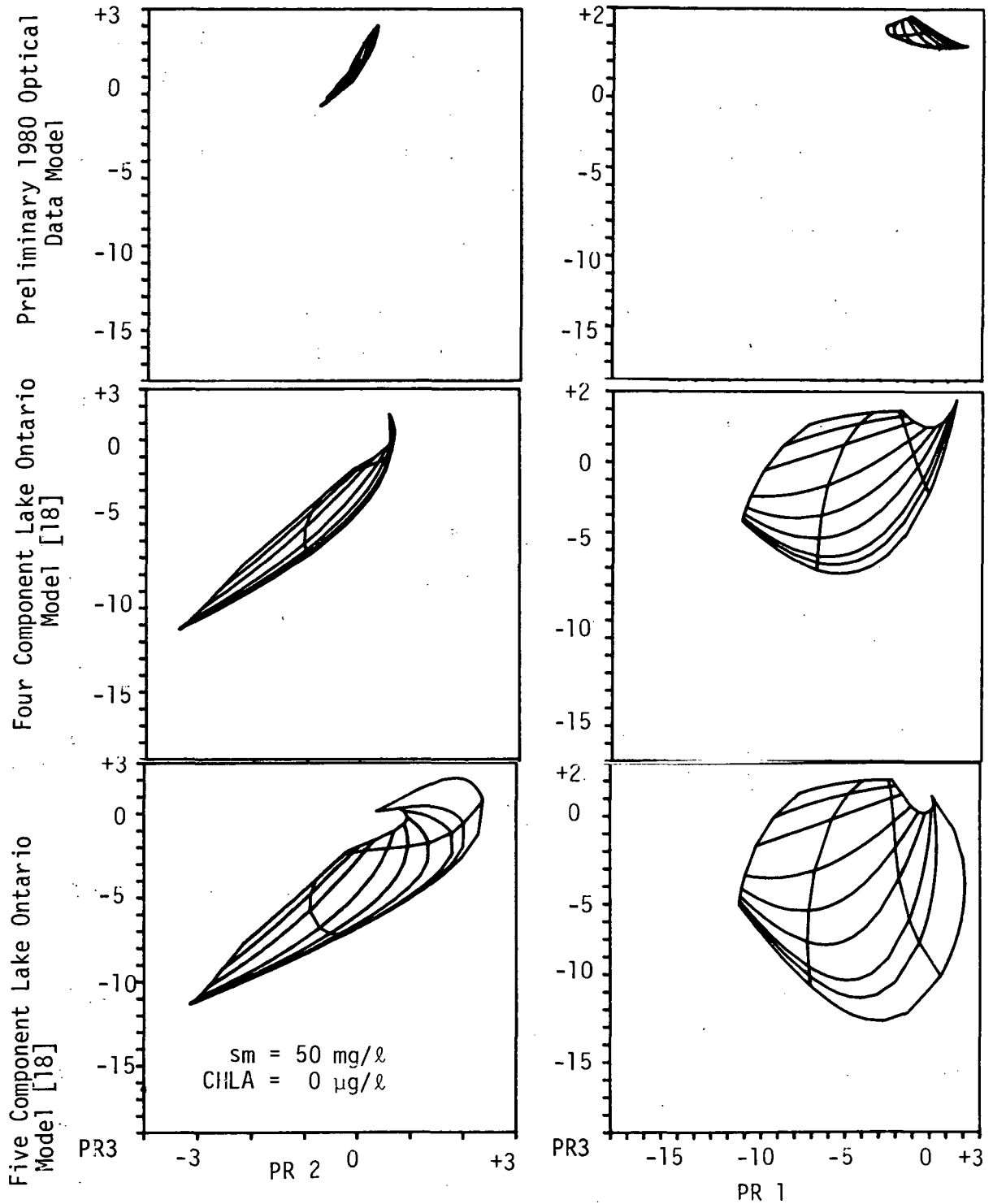


Figure 6. Projected subsurface reflectances (percent) as predicted by each of the above reflectance models. Projected variables are linear combinations of the corresponding predicted CZCS reflectances as shown in Figures 3, 4, and 5.

- (2) Fixed chlorophyll, variable sediment, fixed haze, zero system noise;
- (3) Variable chlorophyll, variable sediment, variable haze condition, standard system noise level.

The simulations included the effects of system noise by adding a normally distributed random variable with standard deviation equal to the mean radiance divided by the signal-to-noise ratio. The signal-to-noise ratio used were those reported by Gordon for CZCS [1]. The preliminary algorithms derived from these simulation data sets use as a first step the atmospheric projection procedure described in section 3.4. The orientation of the atmospheric vector was that given in Table 5. Data set (1) as described above was then used to derive a prediction function of the form given in equation (13). Similarly data set (2) was used to derive a corresponding equation for sediment. The third type of data sets (3) were used subsequently to test performance of the derived prediction equations.

Results of these analyses are summarized as follows:

1. Sediment equations for the Lake Ontario models were able to predict sediment concentrations under conditions of variable haze and system noise to within approximately 50% over wide ranges of concentrations (1 to 20 mg/l) and to within 30% over narrow ranges (1 to 5 mg/l).
2. The sediment equation for the preliminary 1980 optical model were able to predict sediment concentration to less than 50% only after the signal-to-noise ratio was doubled.
3. None of the regression equations for chlorophyll were capable of predicting chlorophyll to within 50% under standard system noise conditions. When the noise was reduced by four times the

Lake Ontario optical model predictions fell within the 50% error range. The presence of sediment, as might be expected, was found to have a deteriorating effect on the prediction algorithms for chlorophyll.

4. Satisfactory results were obtained with the preliminary 1980 optical model only when the presence of sediment was reduced to very small quantities ( $\ll 1$  mg/l) and the system noise was virtually eliminated.

While we are encouraged by these simulation results additional investigations of this type will be needed under Phase II in order to produce satisfactory algorithms. The simulation techniques developed in the present study will become a powerful analytical tool for investigating and evaluating the applicability of Phase II CZCS algorithms to the Great Lakes.

Attempts to apply derived chlorophyll and sediment algorithms to Great Lakes CZCS data sets were not viable because of the lack of surface truth. However, some preliminary analysis was performed on the May 8, 1979 scene. The derived atmospheric vector compared well with that obtained from the atmospheric model as discussed in the previous section.

The processing portions of the final algorithm is anticipated to be able to classify the image and separate it into a land and water file. The water file, which will contain the surface area of the Great Lakes, will be then radiometrically calibrated in the first four bands. In turn, the water file will be transformed to one suitable for constituent determinations by projecting the data along the atmospheric vector. Applying the sediment and chlorophyll prediction equations to the projected file will produce the desired pixel by pixel concentrations maps. These concentration data files would then be recombined in the computer with the land mass file to produce a final map product.

A first attempt at performing some of these manipulations was made for the May 8, 1979 scene. While complete processing was beyond the scope of the present program phase we were able to separate the image into land and water files, color slice the water file, and recombine the separated image as shown in Figure 7.



FIGURE 7. GREAT LAKES CZCS IMAGE FOR MAY 8, 1979 RECONSTRUCTED FROM WATER AND LAND FILES. In this image the water is represented by a CZCS band 4 (670 nm) level slice depicting sediment concentration. The land area is shown as continuous grey tone image of band 5 (750 nm). It should be noted that the original image was color coded and, therefore, the dark areas of the lakes as seen above do not accurately represent the quantity of sediment present.

## SUMMARY AND CONCLUSIONS

Much of the work accomplished to date is preliminary to the validation of CZCS in the Great Lakes. During the first phase of an anticipated two phase program, efforts were initiated and directed toward development of the necessary algorithms and supporting processing software which will allow the transformation of CZCS images of the Great Lakes into maps depicting concentrations of chlorophyll-a and sediment. The second phase will involve analyses of the CZCS imagery and surface truth measurements collected during the 1980 summer experiments.

Preliminary examination of existing CZCS atmospheric correction algorithms developed by NOAA for the open ocean indicates that the assumptions required are not valid for much of the Great Lakes area. Work has begun on the development of new atmospheric correction algorithms which are appropriate to the Great Lakes. While these algorithms appear to be promising, they have not as yet been thoroughly tested with actual CZCS data.

A preliminary optical model was derived from the LaRC optical measurements made for Great Lakes waters. Derived chlorophyll-a cross sections were found to be less than those reported with the Lake Ontario models [18] and elsewhere in the literature.

Efforts to derive chlorophyll and suspended sediment algorithms were based upon simulations of the preliminary optical model and the Lake Ontario models. Simulations included system noise and atmospheric variants as calculated using existing models. Multiple non-linear regression techniques were used to derive water quality prediction equations from Great Lakes CZCS simulation data. While results produced are encouraging they are thus far incomplete because of the lack of sufficient optical data and appropriate CZCS images. Suspended sediment algorithms were found to be able to predict sediment concentrations with

single pixel accuracy to within 50% of the true value over the range (1-20 mg/l) for all optical models under consideration. Chlorophyll on the other hand was found to be more difficult to predict because of its smaller optical cross section. A 50% prediction accuracy could only be obtained after substantial reduction was made to the system signal to noise ratios. Furthermore this improvement was only realized with the Lake Ontario optical models. Satisfactory chlorophyll predictions could not be obtained using the preliminary optical model for the Great Lakes. This result was anticipated in part since the derived chlorophyll optical cross sections were much smaller than expected.

A second activity of the current work involved development of a geometric correction algorithm for CZCS. A scanner model specific to CZCS was developed which accounts for image distorting scanner and satellite motions. This model was used in turn to generate mapping polynomials that define the transformation from the original image to one configured in a polyconic projection.

Actually two approaches were investigated in the present study to obtain these mapping polynomials; geometric regression and orbit modeling. Based on a single available CZCS scene for the Great Lakes a geometric regression of anchor points produced mapping polynomials which predicted the location of ground control points with RMS errors of approximately five pixels in both the horizontal and vertical directions. By comparison the scanner model produced RMS errors of less than one pixel in the horizontal and 1.5 pixels in the vertical directions. Thus the scanner model approach is presently considered to be superior to exclusive use of image anchor points.

While some minor modifications to the scanner model are anticipated as additional imagery is acquired the software package to provide CZCS geometric correction is essentially complete.

## REFERENCES

1. Gordon, H.R., et al., Phytoplankton Pigments from the Nimbus-G Coastal Zone Color Scanner: Comparisons with Surface Measurements, Science, Vol. 210, October 3, 1980.
2. Hovis, H.R. and Leung, K.C., Optical Engineering, Vol. 16, pg. 157, 1977.
3. Quenzel, H. and M. Kaestner, Optical Properties of the Atmosphere: Calculated Variability and Application to Satellite Remote Sensing of Phytoplankton, Applied Optics, Vol. 19, No. 8, April 1980.
4. Polcyn, F.C. and I.J. Sattinger, Marine Ecosystems Analysis Program: A Summary of Remote Sensing Investigations in the New York Bight, NOAA Contractor Report 131200-1-F, Environmental Research Institute of Michigan, March 1979.
5. Wezernak, C.T., The Use of Remote Sensing in Limnological Studies, Proceedings, Ninth International Symposium on Remote Sensing of Environment, Ann Arbor, pp. 963-980, 1974.
6. Wezernak, C.T., Satellite Remote Sensing Study of the Trans-Boundary Movement of Pollutants, EPA-600/3-77-056, U.S. Environmental Protection Agency, Duluth, Minnesota, May 1977.
7. Gordon, H.R., Removal of Atmospheric Effects from Satellite Imagery of the Oceans, Applied Optics, Vol. 17, No. 10, 15 May 1978.
8. Austin, R.W., Scripps Institution of Oceanography. Personal Communication, February 1981.
9. Wolford, G.N., Nimbus Observation Processing System (NOPS) Tape specification T744041 for CZCS NASA/GSFC, May 5, 1980.
10. Coney, Thom A. and Salzman, Jack A., A Comparison of Measured and Calculated Upwelling Radiance Over Water as a Function of Sensor Altitude, Proceedings, Thirteenth International Symposium on Remote Sensing of the Environment, p. 1707, 1979.
11. Tanis, F.J., Polcyn, F.C., and Doak, E.L., Measurement of Sea Surface Upwelling Radiance in the Gulf of Mexico Using the Nimbus-G Coastal Zone Color Scanner, Proceedings Fourteenth International Symposium on Remote Sensing of Environment, p. 1859, 1980.
12. Dave, J.V., Subroutines for Computing the Parameters of Electromagnetic Radiation Scattered by a Sphere, IBM Report 320-3237, (IBM Scientific Center, Palo Alto, California, 1968).



13. Bukata, R. P., et al., Optical Water Quality Model of Lake Ontario 1: Determination of Optical Cross Sections of Organic and Inorganic Particulates in Lake Ontario. Applied Optics, Vol. 20, No. 9, May 1, 1981.
14. Gordon, H.R., Brown, O.B., and Jacobs, M.M., Computed Relationships Between Inherent and Apparent Optical Properties of a Flat Homogeneous Ocean, Applied Optics, Vol. 14, p. 417, February 1975.
15. Elterman, L., Vertical-Attenuation Model with Eight Surface Meteorological Ranges 2 to 13 kilometers, Report No. AFCRL-70-200, Air Force Cambridge Research Laboratories, Office of Aerospace Research, Bedford, Mass., 1970.
16. Whitlock, Charles, et al., Comparison of Reflectance with Backscatter and Absorption Parameters for Turbid Waters. Applied Optics, Vol. 20, No. 3, pg. 517, February 1, 1981.
17. Reyner, Eric, 1980 CZCS Sea-Truth Data, Personal Communication to members of the GLET, May 1981.
18. Bukata, R.P., et al., Optical Water Quality Model of Lake Ontario 2: Determination of Chlorophyll-a and Suspended Mineral Concentrations of Natural Waters from Submersible and Low Altitude Optical Sensors, Applied Optics, Vol. 20, No. 9, May 1, 1981.
19. Hodgkinson, J.R. and Greenleaves, I., Computations of Light-Scattering and Extinction by Spheres According to Diffraction and geometric Optics, and Some Comparisons with Mie Theory., Proc. of Optical Society of America, Vol. 53, No. 5, May 1963.
20. Van De Hulst, H.C., Light Scattering by Small Particles, Wiley, New York, New York, 1957.

## APPENDIX A

## CZCS GEOMETRIC CORRECTION SOFTWARE

This appendix contains FORTRAN IV listings of four programs as developed for the PDP-11/70 computer system under the present contract. These programs form the basis of ERIM's present capability to transform NASA/GSFC CZCS image files into an image with desired metric qualities. The four programs include: (1) the CZCS Scanner Model, (2) CZCS Image Ground Control Program, (3) the Mapping Projection Polynomial Generation Program, and (4) an adapted Nearest Neighbor Resampling Program. These programs do not constitute a stand alone capability but instead require selected supporting software from ERIM's Earth Resources Data Center (ERDC) operating system. Available documentation and operating instruction can be obtained by request from ERDC.



COASTAL ZONE COLOR SCANNER MODEL

```

SEQ CZCSMRG.FTN          26-FEB-81  12:44:07  PAGE      1
1.....!.....!.....!.....!.....!.....!.....!.....!.....!.....!.....
10  PROGRAM CZCSMR
20  C  COASTAL ZONE COLOR SCANNER MERGE  "CZCSMRG"
30  C
40  C
50  C
60  C  MODIFIED FROM EDIPSMRG ON AUGUST 27, 1980 BY GLENN DAVIS
70  C  THIS PROGRAM WILL READ A COASTAL ZONE COLOR SCANNER DATA TAPE
80  C  AS DESCRIBED IN "NIMBUS G, NIMBUS OBSERVATION PROCESSING SYSTEM
90  C  (NOPS) TAPE SPECIFICATION T740041 CZCS CRT TAPE, 4/19/79".
100 C  THE HEADER INFORMATION IS EXTRACTED AND COPIED TO THE HEADER FILE.
110 C  THE DATA CHANNELS ARE INTERLEAVED AND COPIED TO THE IMAGE FILE.
120 C
130 C  OPTIONALLY THE ANCHOR POINTS ARE COPIED TO A FILE
140 C
150 C  PARAMETER EOF=1,BEGIMG=861,BEGANC=237,ANCLN=616,ENDANC=852
160 C  PARAMETER ANCREC=150,REGILT = 1549, OFFDAY = 7, OFFSEC = 9
170 C  PARAMETER GRPSZ = 405, SURATT=21,PREATT=69,REGATT= 1705
180 C  PARAMETER NLONSZ=33,NLATSZ=36,NALTSZ=39,POSSZ = 45
190 C  PARAMETER GMTSZ = 18,SECGRP=16,GMTINC=1702
200 C  PARAMETER PITOFF = 0, YAWOFF = 3, ROLOFF = 6
210 C
220 C  INTEGER START,DEGREE,FRAC1,FRAC2,FRAC3,END,WHCANC
230 C  INTEGEN OFFSET, GMTD12, WHCGRP, WHCSEC
240 C  INTEGER*4 NADALT(4), NADTIM(4)
250 C  INTEGER * 4 RESULT,SECNDS,IMGSZ,GMTSEC,LDMIN,HIMIN,WHCMIN
260 C  INTEGER*4 WORK,FRAC,TWO16,TWO8,NADCNT,SPAN,IMGEDG,MINMRK,IMGBEG
270 C  INTEGER UNIT,DEN,RECNR,YEAR,DAY,LATLON(2)
280 C  INTEGER DBUF2(5924),TILTID,TILT,TILTSV,ANS
290 C
300 C
310 C  REAL LT,LN,SDAY12,GSEC
320 C  REAL GEO,TWO22,POINTS(154),OPMR,GTBASE,RTIME
330 C  REAL NADLAT(4), NADLON(4)
340 C  REAL SUMPOL, SUMPIT, SUMYAW, PITRAT, ROLRAT, YAWRAT
350 C  REAL * 8 WORK
360 C
370 C
380 C  LOGICAL*1 LRF(12780),MFN(18),ST(10),ORUF(11808)
390 C  LOGICAL*1 SID(12),HT(30),COORDS(4),SWAP,LOAD
400 C  BYTE ANCHOR,SEC(4)
410 C  EQUIVALENCE ( YEAR,LRF(17)),(SECNDS,LRF(21)),( DAY,LRF(19))
420 C  EQUIVALENCE ( TILT,LRF(17)),(TILTID,LRF(19))
430 C  EQUIVALENCE ( DBUF,DBUF2 ),(IMGSZ,LRF(251)),(GMTSEC,SEC(1))
440 C  EQUIVALENCE (LRF(1),RECNR)
450 C  EQUIVALENCE ( LATLON,COORDS),( RESULT,COORDS)
460 C
470 C
480 C
490 C  OPEN FILES, SET CONSTANTS
500 C
510 C  ASSIGN 99402 TO I99400
520 C  GO TO 99400
530 C 99402 CONTINUE
540 C
550 C  GET FIRST NADIR VALUES
560 C

```

ORIGINAL PAGE IS  
OF POOR QUALITY



APPLICATIONS DIVISION

```

560 CZCSMRG.FTN          26-FEB-81   12144107   PAGE      2
!.....!.....!.....!.....!.....!.....!.....!.....!.....!.....
570          ASSIGN 99802 TO 199800
580          GO TO 99800
590 99802 CONTINUE
600 C
610 C
620 C
630 C      GET FIRST GROUP OF ATTITUDE VALUES
640 C
650 C      ASSIGN 99302 TO 199300
660 C      GO TO 99300
670 99302 CONTINUE
680 C
690      IMGHEG = IMGEDG
700 C
710 C
720 900 CALL READ(UNIT, LRF, 12780, NAR, IC)
730      IF (NAR.NE.12780) GO TO 950
740 C
750      IF (.NOT.(LOAD.OR.ANCHOR)) GO TO 900
760 C
770      SWAP = LRF(1)
780      LRF(1) = LRF(2)
790      LRF(2) = SWAP
800 C
810 D      TYPE 910, RECNR, RECNR
820 0910 FORMAT(15, D6)
830 C
840      RECNR = 971 - ( RECNR/16 ) + 1
850          ! ADD ONE TO MAKE VALUE ONE RELATIVE
860          ! SUBTRACT FROM 971 TO INVERT IMAGE
870          ! DIVIDE BY 16 TO SHIFT RIGHT 4 BITS
880 C
890 C      TYPE 910, RECNR, RECNR
900      TILTID = MOD(TILTID, 256)
910      IF (TILTID.NE.2) GO TO 680
920      SWAP = LRF(17)
930      LRF(17) = LRF(18)
940      LRF(18) = SWAP
950 C
960      IF (TILT.FQ.TILTSV) GO TO 680
970      TILTSV = TILT
980 C      DIVIDE BY 256 TO USE LEFT HALF OF WORD WHICH IS THE WHOLE PART
990 C      OF THE NUMBER
1000     RWORK = FLOAT( TILT / 256 )
1010     TLTVAL = RWORK * -.367 + 29.87
1020 D     WRITE(5, 682) RWORK, TLTVAL, RECNR
1030 682  FORMAT(' TILT = ', F5.0, ' TILT (DEG) = ', F8.4, ' AT RECORD ', I5)
1040     680 CONTINUE
1050 C
1060 C
1070      IF (.NOT.ANCHOR) GO TO 684
1080 C
1090 C      GET LINE OF ANCHOR POINTS
1100 C      ASSIGN 99902 TO 199900
1110 C      GO TO 99902
1120 99902 CONTINUE

```





```

SFO C7CSMRG,FTN 26-FEB-81 12144107 PAGE 4
1690 C
1700 STOP
1710 C
1720 C99901 GO TO 199900,(99902)
1730 C
1740 C99801 GO TO 199800,(99802,99803)
1750 C
1760 C99701 GO TO 199700,(99702,99706,99707,99708,99709)
1770 C99701 GO TO 199700,(99706,99707,99708)
1780 C
1790 C99601 GO TO 199600,(99602)
1800 C
1810 C99501 GO TO 199500,(99502,99503,99504,99505)
1820 C
1830 C99401 GO TO 199400,(99402)
1840 C
1850 C99301 GO TO 199300,(99302)
1860 C
1870 C99201 GO TO 199200,(99202)
1880 C
1890 C99101 GO TO 199100,(99102,99103,99104)
1900 C
1910 C99001 GO TO 199000,(99002)
1920 C
1930 C*****
1940 C
1950 C GET ANCHOR POINTS
1960 C
1970 C99900 CONTINUE
1980 C
1990 C LONGITUDES MUST BE CONVERTED FROM 0 TO 360 SYSTEM TO +/- 180 DEG.
2000 C
2010 C
2020 C EACH GEOGRAPHIC COORDINATE OCCUPIES FOUR BYTES.
2030 C BIT 31 REPRESENTS THE SIGN
2040 C BITS 30-22 REPRESENT THE WHOLE DEGREES PORTION OF THE NUMBER.
2050 C BITS 21-0 REPRESENT THE SEVEN-DIGIT DECIMAL FRACTION OF DEGREES.
2060 C
2070 C SINE = LBF ( WHCANC ) .AND. "200 ! SIGN IS ALWAYS POSITIVE
2080 C SINE = ISIGN(1, SINE )
2090 C
2100 C
2110 C WHCPNT = 0
2120 C
2130 C DO 982 WHCANC = BEGANC,ENDANC,4
2140 C
2150 C
2160 C DEGREE = LBF ( WHCANC ) .AND. "177
2170 C DEGREE = ISHFT(DEGREE,2)
2180 C WORK = LBF ( WHCANC + 1 ) .AND. "300
2190 C WORK = WORK / 64 ! SHIFT 6 BITS TO RIGHT
2200 C
2210 C DEGREE = DEGREE + WORK
2220 C
2230 C FRAC1 =LBF ( WHCANC + 1 ) .AND. "077
2240 C

```



```
SEQ CZCSMRG,FTN 26-FEB-81 12144107 PAGE 5
|.....|.....|.....|.....|.....|.....|.....|.....|.....|.....|.....
2250 C FRAC2 =LBF ( WHCANC + 2 ) ,AND, "377
2260 C
2270 C FRAC3 =LRF ( WHCANC + 3 ) ,AND, "377
2280 C
2290 C END = WHCANC + 3
2300 C
2310 D TYPE 931,WHCANC,(LBF(I),I=WHCANC,END),(LBF(I),I=WHCANC,END)
2320 D931 FORMAT( ' POINT ',I5,2X,' DEC: ', 4(I6,1X)
2330 D + ',/,14X,' OCT: ',4(D6,1X) )
2340 C
2350 C FRAC = FRAC1 + TWO16 + FRAC2 * TWO8 + FRAC3
2360 C
2370 C RWORK = FLOAT ( FRAC ) / ( TWO22 )
2380 C
2390 C GEO = FLOAT(DEGREE ) + RWORK
2400 C
2410 C IF (GEO.GT.180) GEO = - (360. - GEO )
2420 C
2430 D TYPE 930,DEGREE,FRAC1,FRAC2,FRAC3,FRAC,RWORK,TWO22
2440 C930 FORMAT( 4(I6,1X),I10,F15,12,F10,2)
2450 C
2460 D TYPE 932, GEO
2470 C932 FORMAT( 1X, F12,8)
2480 C
2490 C WHCPNT = WHCPNT + 1
2500 C POINTS(WHCPNT) = GEO
2510 C
2520 C992 CONTINUE
2530 C
2540 C
2550 C WRITE(3'RECNR) ( POINTS(K),K=1,WHCPNT)
2560 C685 FORMAT( < WHCPNT > F9,4 )
2570 C
2580 C
2590 C
2600 C GO TO 99901
2610 C*****
2620 C
2630 C PROCEDURE TO EXTRACT NADIR INFORMATION
2640 C
2650 C
2660 C99800 CONTINUE
2670 C
2680 C
2690 C GET GMT IMAGE EDGE (IMGEDG) AND LENGTH OF IMAGE (SPAN )
2700 C
2710 C SWITCH BYTES AND WORDS TO MATCH DEC CONVENTIONS
2720 C
2730 C DO 90 WORK = 21,25,4
2740 C
2750 C SWAP = LBF(WORK)
2760 C LRF( WORK ) = LBF( WORK + 3 )
2770 C LRF( WORK + 3 ) = SWAP
2780 C
2790 C SWAP = LBF(WORK + 1 )
2800 C LRF( WORK + 1 ) = LBF( WORK + 2 )
```











```

SEQ  CZCSMRG,PTN      26-FEB-81  12144107  PAGE  9
4490  C
4500  C      CONSTANTS FOR HEADER FILE
4510  C
4520  NE=1968          | NUMBER OF OUTPUT ELEMENTS
4530  NL=970          | NUMBER OF OUTPUT LINES
4540  NBP=6           | NUMBER OF BYTES/PIXEL
4550  IPN=5           | PROJECTION NUMBER
4560  NPP=0           | NUMBER OF PROJECTION PARAMETERS
4570  IEO=0           | ELEMENT OFFSET
4580  ILO=0           | LINE OFFSET
4590  NOVL=6          | NUMBER OF OVERLAYS
4600  DX=825          | SAMPLING INTERVAL (METERS) ACROSS TRACK
4610  DY=825          | SAMPLING INTERVAL (METERS) ALONG TRACK
4620  C
4630  NR=NE*NBP
4640  C
4650  IF (LOAD) CALL IMOPEN(1,ST,,IDR,NB,NL,'M')
4660  OPEN ( UNIT = 4, NAME = 'CSP.DAT',TYPE='NEW')
4670  C
4680  GO TO 99401
4690  C
4700  C*****
4710  C
4720  C
4730  C      LOAD HEADER FILE
4740  C
4750  99400 CONTINUE
4760  C
4770  CALL GFN (ST,HFN)
4780  CALL ASSIGN (1,HFN)
4790  C
4800  C
4810  CALL MOVE(LRF(33),1,COORDS(1),1,4,0)
4820  C
4830  C
4840  SWAP = COORDS(2)
4850  COORDS(2) = COORDS(1)
4860  COORDS(1) = SWAP
4870  C
4880  SWAP = COORDS(4)
4890  COORDS(4) = COORDS(3)
4900  COORDS(3) = SWAP
4910  C
4920  C
4930  LATLON(1) = LATLON(1) - 9000
4940  IF (LATLON(2).GT.18000) LATLON(2) = - ( 36000 - LATLON(2) )
4950  LT = FLOAT(LATLON(1)) / 100
4960  LN = FLOAT(LATLON(2)) / 100
4970  C
4980  C
4990  WRITE (1,150) YEAR,DAY,HT
5000  150  FORMAT(1X,I4,' ',I3,2X,30A1,7X)
5010  C
5020  C
5030  WRITE (1,160) NE,NL,NBP,IPN,NPP,IEO,ILO,NOVL
5040  160  FORMAT (8I5,40X)

```















```
SEQ      C,FTN      26-FEB-81  12147111  PAGE      4
1690     .....1.....1.....1.....1.....1.....1.....1.....1.....1.....1.....1.....
1700     CALL SAR(X4,Z4,-FF,X5,Z5)
1710     Y5=Y4
1720     CALL SAR(Y5,X5,TH,Y6,X6)
1730     Z6=Z5
1740     CALL SAR(X6,Z6,-TS,X7,Z7)
1750     Y7=Y6
1760     CALL SAR(X7,Y7,-HL,X2,Y2)
1770     Z2=Z7
1780     CALL SAR (Z2,Y2,PT,Z3,X3)
1790     CALL SAR (Y2,Z3,HD,Y4,Z4)
1800     CALL SAR (Z4,X3,GCLT,Z5,X5)
1810     CALL SAR (Y4,X5,LN,Y6,X6)
1820     C
1830     AQ=X6*X6+Y6*Y6+Z5*Z5+ECS
1840     BQ=2,*(X6*X0+Y6*Y0+Z5*Z0+ECS)/AQ
1850     T0,5=(-BQ-SQRT(BQ*BQ-4,*C/AQ))
1860     XE=X6*T+X0
1870     YE=Y6*T+Y0
1880     ZE=Z5*T+Z0
1890     LILP=ATAN(ZF+ECS/SQRT(XE*XE+YE*YE))
1900     LNLP=DPR*ATAN2(YE,XE)
1910     LTLP=DPR*LTLP
1920     ELT=LTLP-PLT(ICP)
1930     ELN=LNLP-PLN(ICP)
1940     WT=1W(ICP)
1950     ENI=ELT*RE/DPR
1960     EEI=ELN*RE*CLT/DPR
1970     CALL SAR (ENI,EEI,HD,PTE,RLE)
1980     RLE=RLE*COS(TH)
1990     X(1)=RLE
2000     X(2)=ST
2010     X(3)=ST*ST
2020     X(4)=ST*ST*ST
2030     K=1
2040     DO 260 I=1,4
2050     XR(I)=XB(I)+X(I)*WT
2060     DO 260 J=I,4
2070     A(K)=A(K)+X(I)*X(J)*WT
2080     K=K+1
2090     C
2100     Y(1)=PTE
2110     Y(3)=ST
2120     Y(4)=ST*ST
2130     Y(5)=ST*ST*ST
2140     Y(2)=TH*ALT
2150     C
2160     K=1
2170     DO 270 I=1,5
2180     YR(I)=YB(I)+Y(I)*WT
2190     DO 270 J=I,5
2200     B(K)=B(K)+Y(I)*Y(J)*WT
2210     K=K+1
2220     SW=SW+WT
2230     SSN=SSN+ENI*ENI*WT
2240     SSE=SSE+EEI*EEI*WT
2250     EN(ICP)=ENI
```



```

SEQ      C,PTN      26-FEB-81  12147111  PAGE      5
1.....

2250      EE(ICP)=EEI
2260      CTEW=CTEW+TH*RL
2270      CTEW2=CTEW2+TH*TH*RL
2280      CTNS=CTNS+TH*TH*PTE
2290      280  CONTINUE
2300      C
2310      C
2320      CTEW=CTEW/SW
2330      CTEW2=CTEW2/SW
2340      CTNS=CTNS/SW
2350      K=I
2360      DO 290 I=1,4
2370      DO 290 J=1,4
2380      A(K)=A(K)-XB(I)*YB(J)/SW
2390      290  K=K+1
2400      K=I
2410      DO 300 I=1,4
2420      YB(I)=YB(I)/SW
2430      DO 300 J=1,4
2440      A(K)=A(K)/(SW-1.)
2450      300  K=K+J
2460      DO 310 I=1,4
2470      310  SDX(I)=SQRT(A(LF(4,10,I,I)))
2480      K=I
2490      DO 320 I=1,4
2500      DO 320 J=1,4
2510      A(K)=A(K)/(SDX(I)*SDX(J))
2520      320  K=K+J
2530      DO 330 I=2,1+IDG
2540      IF (A(LF(4,10,I,I)),LT,1.E-5) GO TO 740
2550      330  CALL STEP (A,10,4,I)
2560      C
2570      Y(I)=YB(I)
2580      DO 340 I=2,1+IDG
2590      Y(I)=SDX(I)*A(LF(4,10,I,I))/SDX(I)
2600      340  Y(I)=X(I)-X(I)*YB(I)
2610      DO 350 I=1,1+IDG
2620      350  R(I)=R(I)+X(I)
2630      C
2640      K=I
2650      DO 360 I=1,5
2660      DO 360 J=1,5
2670      R(K)=R(K)-YB(I)*YB(J)/SW
2680      360  K=K+J
2690      K=I
2700      DO 370 I=1,5
2710      YB(I)=YB(I)/SW
2720      DO 370 J=1,5
2730      R(K)=R(K)/(SW-1.)
2740      370  K=K+J
2750      DO 380 I=1,5
2760      380  SDY(I)=SQRT(B(LF(5,15,I,I)))
2770      K=J
2780      DO 390 I=1,5
2790      DO 390 J=1,5
2800      R(K)=R(K)/(SDY(I)*SDY(J))

```



ORIGINAL PAGE IS  
OF POOR QUALITY



APPLICATIONS DIVISION

```

350 C,PTN 26-FEB-81 12147111 PAGE 7
1.....

3370 IF (ITW,GT,10) ITW=10
3380 DO 570 I=1,N
3400 570 CONTINUE
3410 IPWF=1
3420 WRITE (5,500)
3430 580 FORMAT ('$ANOTHER ? ')
3440 GO TO 550
3450 590 IF (IPWF,NE,0) GO TO 230
3460 WRITE (5,600)
3470 600 FORMAT ('$ OUTPUT ON LINE PRINTER ? ')
3480 READ (5,605) LPA
3490 605 FORMAT(A1)
3500 IF (LPA,NE,AY) GO TO 610
3510 LP=6
3520 GO TO 445
3530 610 WRITE (5,620)
3540 620 FORMAT ('$PRINTER PLOTS ? ')
3550 READ (5,605) LPA
3560 IF (LPA,NE,AY) GO TO 720
3570 C
3580 WRITE (5,630)
3590 630 FORMAT ('$METERS PER DIVISION ? ')
3600 HEAD (5,30) PPS
3610 IF (PPS,EG,0.) PPS=200.
3620 PPSF=PPS/10.
3630 WRITE (6,640) PPS
3640 640 FORMAT ('PIXEL V.S. ERRORS',T28,'EAST',T88,'NORTH',F10.0,'METERS/
3650 10IV')
3660 DO 670 I=1,60
3670 LL=(I-1)*33
3680 LU=I*33
3690 DO 660 J=1,N
3700 IF (IW(J),EQ,0) GO TO 660
3710 IF (IX(J),LE,LL) GO TO 660
3720 IF (IX(J),GT,LU) GO TO 660
3730 IEE=EE(J)/PPSF+30.
3740 IEN=EN(J)/PPSF+90.
3750 IF (IEE,LT,2) IEE=2
3760 IF (IEE,GT,60) IEE=60
3770 IF (IEN,LT,61) IEN=61
3780 IF (IEN,GT,120) IEN=120
3790 WRITE (6,650) IPT(J),IPT(J)
3800 650 FORMAT ('+',T<IEE>,I2,T<IEN>,I2)
3810 660 CONTINUE
3820 670 WRITE (6,680)
3830 680 FORMAT (5(9X,' '),10X,5(9X,' '))
3840 WRITE (6,690)
3850 690 FORMAT ('LINE V.S. ERRORS',T28,'EAST',T88,'NORTH')
3860 DO 710 I=1,60
3870 LL=(I-1)*17
3880 LU=LL+17
3890 DO 700 J=1,N
3900 IF (IW(J),EQ,0) GO TO 700
3910 IF (IY(J),LE,LL) GO TO 700
3920 IF (IY(J),GT,LU) GO TO 700

```



```
SEQ C,FTN 26-FEB-81 12147111 PAGE 8
.....
3930 IEE=EE(J)/PPSF*30
3940 IEN=EN(J)/PPSF*90
3950 IF (IEE,LT,2) IEE=2
3960 IF (IEE,GT,60) IEE=60
3970 IF (IEN,LT,61) IEN=61
3980 IF (IEN,GT,120) IEN=120
3990 WRITE (6,650) IPT(J),IPT(J)
4000 700 CONTINUE
4010 710 WRITE (6,680)
4020 720 WRITE (4,730) P(1),P(3),P(4),P(5)
4030 WRITE (4,730) R
4040 WRITE (4,730) P(2)*1,E6
4050 730 FORMAT (6F10,3)
4060 CLOSE(UNIT=6,DISPOSE='PRINT')
4070 STOP
4080 740 WRITE (5,750)
4090 750 FORMAT (' GCP DATA NOT SUITABLE FOR DEGREE SELECTED')
4100 STOP
4110 END
4120 SUBROUTINE LGR( V , FV , XI , XRESLT)
4130 C
4140 C-----
4150 C
4160 C FNVAL1 =
4170 C XRESLT = FNVAL3 =
4180 C FNVAL4 =
4190 C FNVAL2 =
4200 C
4210 C
4220 C
4230 C VAL1 = XINTRP = VAL2 = VAL3 = VAL4 =
4240 C
4250 C GIVEN FOUR VALUES ( VAL1 -> 4 OR ARRAY V ) AND
4260 C GIVEN FOUR CORRESPONDING VALUES ( FNVAL1 -> 4 OR ARRAY FV ) THAT
4270 C ARE A FUNCTION OF THE FORMER VALUES,
4280 C AND GIVEN A VALUE XINTRP ( XI ) THAT IS ADJACENT TO VAL1 -> 4
4290 C THEN THIS ROUTINE RETURNS A VALUE, XRESLT, THAT IS THE LAGRANGE
4300 C INTERPOLATION OF XINTRP ABOUT FNVAL1 -> 4.
4310 C
4320 C
4330 C
4340 REAL V(4) , FV(4) , XRESLT , XI , PART(4)
4350 REAL A,B,C,D
4360 C
4370 A = XI - V(1)
4380 B = XI - V(2)
4390 C = XI - V(3)
4400 D = XI - V(4)
4410 D
4420 D TYPE 500,A,B,C,D
4430 D 500 FORMAT(4F12,5)
4440 D TYPE 500,V
4450 D TYPE 500,FV
4460 D TYPE 500,XI
4470 C
4480 PART(1) = ( B * C * D )
```





MAPPING PROJECTION POLYNOMIAL GENERATION PROGRAM

```

100  SE0  CZSMP,FTN          26-FEB-81  12144128  PAGE    1
100  1.....1.....1.....1.....1.....1.....1.....1.....1.....
100  10  C      COASTAL ZONE SCANNER MAPPING POLYNOMIALS
100  20  C      ADAPTED FROM HMP BY GLENN DAVIS ON JANUARY 13, 1981
100  30  C
100  40          LOGICAL ADVFL
100  50          DOUBLE PRECISION X,XN,A
100  60          DOUBLE PRECISION XMEAN,STDEV,POS0
100  70          DIMENSION Y(40), A(840), C(40), P(40), FE(40)
100  80          DIMENSION XMEAN(40), STDEV(40), B(40), D(40), TOLEV(40), R(40), NI
100  90          IEN(40), INEN(40)
100 100          DIMENSION TT(4),TLT(4),TLN(4),TALT(4)
100 110          INTEGER SID(5),AY,PPF
100 120          LOGICAL*1 IT(10),HFN(18),TM(8),DA(9)
100 130          REAL LT,LN,LTLP,LNLP,LTSC,LNSC,PT,RL,LTSH,LNSH,SF
100 140          REAL LTD,LND
100 150          DIMENSION PS(2),PITCH(5),ROLL(4),DELTA(2)
100 160          COMMON X,XN,A,C,F,FE,L,NTGC,IP,NIP,FINC,FOUT,KAY,FLAG,KOEP,DF,TOL
100 170          DATA RE,RP,DPR,SF/6378200.,6356800.,57.2957795,1000000./
100 180          DATA RMVE/4HRMVE/,ENTR/4MENTR/
100 190          DATA AY/'Y'/
100 200          LF(IY,JX)=JX-IX+NIP+1-(((IP-IX+1)*(IP-IX+2))/2
100 210          ADVFL=.TRUE.
100 220          KB=5
100 230          LP=3
100 240          CALL ASSIGN(3,'CZSMP,LST')
100 250          WRITE (KH,20)
100 260  20  FORMAT ('%COASTAL ZONE SCANNER MAPPING POLYNOMIALS REV 1.0'/
100 270          I'%PROJECTION NUMBER ? ')
100 280          READ (KH,30) IPN,LR
100 290  30  FORMAT (2I10)
100 300          RES=RE*RE
100 310          EC=RE/RP
100 320          ECS=EC*EC
100 330  C
100 340          IALL = 1968
100 350          LLD = IALL / 2
100 360  C
100 370          WRITE (KH,37)
100 380  37  FORMAT ('%IMAGE TITLE ? ')
100 390          READ (KH,31) IT
100 400  31  FORMAT (10A1)
100 410          CALL GHFN (1T,HFN)
100 420          CALL ASSIGN (2,HFN)
100 430          READ (2,32) SID
100 440  32  FORMAT (1X,5A2)
100 450          READ (2,33) NTE,NIL,NBP,IIP,NIPP,IEO,ILO
100 460  33  FORMAT (7I5)
100 470          READ (2,34) DELTA(1),DELTA(2),LTSC,LNSC
100 480  34  FORMAT (4F12,6)
100 490          CALL CLOSE (2)
100 500          CALL GT(LTSC,LNSC,IPN,U0,V0)
100 510  C
100 520          CALL ASSIGN(4,'CSP,DAT')
100 530          READ (4,40) SID
100 540  40  FORMAT(5A2)
100 550          WRITE(5,40)SID
100 560          READ (4,50)T0

```

ORIGINAL PAGE IS  
OF POOR QUALITY



APPLICATIONS DIVISION

```

SEQ  CZ5MP,FTN          26-FEB-81  12144128  PAGE  2
1.....|.....|.....|.....|.....|.....|.....|.....
570  50  FORMAT(2F12.6,F12.0,F12.6)
580      DO 60 I=1,4
590      READ(4,50)TLT(I),TLN(I),TALT(I),TY(I)
600      60  WRITE(5,50)TLT(I),TLN(I),TALT(I),TY(I)
610      READ(4,50)TILT
620      READ (4,730) PITCH(1),PITCH(3),PITCH(4),PITCH(5)
630      READ (4,730) ROLL
640      READ (4,730) PITCH(2)
650      730  FORMAT(6F10.3)
660      CALL CLOSE (4)
670      TS=NINT(TILT)/(2.*DPR)
680      FF=45./DPR
690      C
700      C
710      IP=21
720      NIP=(IP*(IP+1))/2
730      CALL ALTPRI(,45)
740      C
750      CALL ASSTGN (1,"COEF,GEO")
760      WRITE (1,100) SID,IPN
770      100  FORMAT (5A2,I10)
780      C
790      CALL DATE (DA)
800      CALL TIME (TM)
810      WRITE (1,110) DA,TM
820      110  FORMAT (1X,9A1,2X,8A1)
830      WRITE (LP,120) DA,TM
840      C
850      120  FORMAT ('COASTAL ZONE SCANNER MAPPING POLYNOMIALS '9A1,2X,8A1//)
860      WRITE (LP,130) SID,IPN
870      130  FORMAT (' SCENE ID ' ,5A2,' PROJECTION NUMBER',I4)
880      C
890      WRITE(KB,251)
900      251  FORMAT('SLNSH,LTSH,VM,TILT ? ')
910      READ(KB,252) LNSH,LTSH,VM,YS
920      252  FORMAT(4F10.0)
930      TS = TS / DPR
940      C
950      C
960      C  INITIALIZE ACCUMULATORS AND MATRIX A
970      C
980      DO 660 I=1,2
990      M=0
1000     DO 140 I=1,IP
1010     XMEAN(I)=0.
1020     DO 140 J=1,IP
1030     M=M+1
1040     140  A(M)=0.
1050     C
1060     N=0
1070     C
1080     DO 180 INS = 1 , 27
1090     TY = (INS-14) * 35 + 485
1100     ST = FLOAT ( TY ) * 485.  | NORMALIZE ALONG TRACK DIMENSION
1110     ST = ST /485.            | NORMALIZE ALONG TRACK DIMENSION
1120     C

```





```

1000 C23MP,FTN          26-FEB-81  12144128  PAGE    3
1130 1.....!.....!.....!.....!.....!.....!.....!.....!.....!.....!.....
1140 T=(970,-IY)*128/(970,*60,)*T0
1150 CALL LGR(TT,TLT,T,LTD)
1160 CALL LGR(TT,TLN,T,LND)
1170 CALL LGR(TT,TALT,T,ALT)
1180 IF (LR,LT,3) GOTO 142
1190 WRITE(5,50)LTD,LND,ALT,FLOAT(IY)
1200 142 CONTINUE
1210 C
1220 LT = LTD / DPR
1230 LN = LND / DPR
1240 LN=LN+LNSH
1250 LT=LT+LTSH
1260 SLT=SIN(LT)
1270 CLT=COS(LT)
1280 SH=,15839/CLT
1290 CH=-SQRT(1,-9H*SH)
1300 HD=ATAN2(SH,CH)
1310 HD=HD+YW
1320 HD=HD+DPR
1330 C
1340 AL=ATAN(SLT/(EC*CLT))
1350 RAL=RE*COS(AL)+ALT*CLT
1360 X0=RAL*COS(LN)
1370 Y0=RAL*SIN(LN)
1380 Z0=HP*SIN(AL)+ALT*SLT
1390 C0=RAL*RAL+Z0*Z0*EC*-HEB
1400 GCLT=ATAN(Z0/RAL)
1410 C
1420 C
1430 PL=,00
1440 RL=RL+(((ROLL(4)*ST+ROLL(3))*ST+ROLL(2))*ST+ROLL(1))/ALT
1450 PT=,0
1460 PI=PI+(((PITCH(5)*ST+PITCH(4))*ST+PITCH(3))*ST+PITCH(1))/ALT
1470 HD=HD-PITCH(2) / SF
1480 C
1490 DO 180 IFW = 1 , 27
1500 IX = (IEW-14) * 70 + 984
1510 PN = IX - LLO
1520 TH=PN*VM/SF
1530 X1=0,
1540 Y1=0,
1550 Z1=ALT
1560 CALL SAR(X1,Z1,TS,Y2,Z2)
1570 Y2=Y1
1580 CALL SAR(Y2,X2,-TH,Y3,X3)
1590 Z3=Z2
1600 CALL SAR(X3,Z3,FF,X4,Z4)
1610 Y4=Y3
1620 X4=-X4      |MIRROR REFLECTION
1630 CALL SAR(X4,Z4,-FF,X5,Z5)
1640 Y5=Y4
1650 CALL SAR(Y5,X5,TH,Y6,X6)
1660 Z6=Z5
1670 CALL SAR(X6,Z6,-TS,X7,Z7)
1680 Y7=Y6
1690 CALL SAR(X7,Y7,-RL,X2,Y2)

```



```
      SEQ      CZ3MP,FTN      26-FEB-81      12144128      PAGE      4
      !.....!.....!.....!.....!.....!.....!.....!.....!.....!.....!.....!.....
1690      Z2=27
1700      CALL SAR (Z2,X2,PT,Z3,X3)
1710      CALL SAR (Y2,Z3,HD,Y4,Z4)
1720      CALL SAR (Z4,X3,GCLT,Z5,X5)
1730      CALL SAR (Y4,X5,LN,Y6,X6)
1740      C
1750      AQ=X6*X6+Y6*Y6+Z5*Z5+ECS
1760      HQ=2*(X6*X0+Y6*Y0+Z5*Z0+ECS)/AQ
1770      T=.5*(-HQ-SQRT(HQ*HQ-4.*C0/AQ))
1780      XE=X6*T+X0
1790      YE=Y6*T+Y0
1800      ZE=Z5*T+Z0
1810      LTLP=ATAN(ZE+ECS/SQRT(XE*XE+YE*YE))
1820      LNLP=DPR*ATAN2(YE,XE)
1830      LTLP=DPR*LTLP
1840      CALL GT (LTLP,LNLP,IPN,U,V)
1850      U=(U-U0)/SF
1860      V=(V-V0)/SF
1870      C
1880      IF (LR.GT.2) WRITE(KB,168) LTLP,LNLP,U,V
1890      168  FORMAT( 2F12.3,2F12.6)
1900      C
1910      K=1
1920      UI=1.
1930      DO 175 I=1,6
1940      VJ=1.
1950      DO 170 J=I,6
1960      X(K)=UI*VJ
1970      VJ=VJ+V
1980      170  K=K+1
1990      175  UI=UI+U
2000      C
2010      IF (ITT.EQ.1) X(I)=IX
2020      IF (ITT.EQ.2) X(I)=IY
2030      N=N+1
2040      M=0
2050      DO 180 J=1,IP
2060      XMEAN(I)=XMEAN(I)+X(I)
2070      DO 180 J=1,IP
2080      M=M+1
2090      A(M)=A(M)+X(I)*X(J)
2100      180  CONTINUE
2110      XN=N
2120      XNT=N
2130      RESDF=XN
2140      M=0
2150      RESDF=XN-1.0
2160      DO 190 I=1,IP
2170      DO 190 J=I,IP
2180      M=M+1
2190      190  A(M)=A(M)-XMEAN(I)*XMEAN(J)/XN
2200      C
2210      C  REPLACE XMEAN WITH MEAN VECTOR, A WITH COVARIANCE MATRIX,AND
2220      C  COMPUTE STANDARD DEVIATIONS
2230      C
2240      M=0
```













SEQ CZSMP,FTN 26-FEB-81 12144128 PAGE 10

```
5050 C  
5060 PART(3) = ( A * B * D )  
5070 + / (( V(3) - V(1)) * ( V(3) - V(2)) * ( V(3) - V(4)) )  
5080 + * FV (3)  
5090 C  
5100 PART(4) = ( A * B * C )  
5110 + / (( V(4) - V(1)) * ( V(4) - V(2)) * ( V(4) - V(3)) )  
5120 + * FV (4)  
5130 XRESLT = PART(1) + PART(2) + PART(3) + PART(4)  
5140 C  
5150 D TYPE 500,PART  
5160 D TYPE 500,XRESLT  
5170 C  
5180 C  
5190 RETURN  
5200 END  
5210 SUBROUTINE STEP  
5220 DOUBLE PRECISION X,XN,A  
5230 DIMENSION X(40), A(800), C(40), F(40), FE(40)  
5240 COMMON X,XN,A,C,F,FE,L,NTGC,IP,NIP,FINC,FOUT,KAY,FLAG,KDEF,DF,TOL  
5250 LF(IY,JX)=JX-IX+NIP+1=((IP-IX+1)*(IP-IX+2))/2  
5260 LKK=LF(KAY,KAY)  
5270 M=0  
5280 DO 70 I=1,IP  
5290 DO 70 J=1,IP  
5300 M=M+1  
5310 IF (I-KAY) 10,70,20  
5320 10 LIK=LF(I,KAY)  
5330 GO TO 30  
5340 20 LIK=LF(KAY,I)  
5350 30 IF (J-KAY) 40,70,50  
5360 40 LKJ=LF(J,KAY)  
5370 GO TO 60  
5380 50 LKJ=LF(KAY,J)  
5390 60 A(M)=A(M)-A(LIK)*A(LKJ)/A(LKK)  
5400 CONTINUE  
5410 DO 110 I=1,IP  
5420 IF (I-KAY) 80,110,90  
5430 80 LIK=LF(I,KAY)  
5440 GO TO 100  
5450 90 LIK=LF(KAY,I)  
5460 100 A(LIK)=A(LIK)*FLAG/A(LKK)  
5470 110 CONTINUE  
5480 A(LKK)=-1.00/A(LKK)  
5490 RETURN  
5500 END
```





CZCS NEAREST NEIGHBOR RESAMPLING PROGRAM

```

SEQ  CZSNR,FTN13          26-FEB-81  12146100  PAGE  1
1.....1.....1.....1.....1.....1.....1.....1.....1.....1.....
10  C  CZCS NEAREST RESAMPLER
20
30  C
40  C  ADAPTED BY GLENN DAVIS ON SEPTEMBER 21, 1980 FROM LNR
50  C
60  C
70  C
80  C
90  PARAMETER NSL=30,NBL=620,MAXOLY=16,BYTRYT=0,WRDHPD=2
100  INTEGER*2 WC,WR
110  INTEGER*2 IOFF(NSL),ID(5), CVAL, START, FIRST
120  LOGICAL*1 LRF(2048),JBUF(NBL,NSL),ST(10),STO(10),HFN(16)
130  LOGICAL*1 PRNTJH, PRNTHD
140  LOGICAL*1 DA(10),TM(10)
150  INTEGER*2 DRN,IV(MAXOLY),NRMVS,MVTYPE,INSKIP,OUTSKP
160  C  NBLTS IS NUMBER OF BLOCKS TO SKIP ON SHORT READ
170  DIMENSION DRVAL(6),DCVAL(6),DR(6),DC(6)
180  REAL LTSC,LNSC
190  C
200  D  CALL ASSIGN( 4,'CZCS,LST')
210  C
220  CALL DATE(DA)
230  CALL TIME(TM)
240  C
250  WRITE (5,20) DA, TM
260  D  WRITE (4,20) DA, TM
270  20  FORMAT ('CZCS NEAREST RESAMPLER V 1.0',4X,10A1,4X,10A1/)
280  NSLM=NSL-1
290  NBL=NBL/2
300  NRTN=NBL+512
310  C
320  C
330  IALL=ALL
340  WRITE (5,30)
350  30  FORMAT ('$INPUT IMAGE TITLE ? ')
360  READ (5,40) ST
370  40  FORMAT (10A1)
380  CALL GHPN (ST,HFN)
390  CALL ASSTGN (2,HFN)
400  READ (2,50) IO
410  50  FORMAT (1X,5A2)
420  READ (2,60) NIE,NIL,NBP,IIP,NIPP,IEO,ILO
430  60  FORMAT (7I5)
440  READ (2,70) DELP,DELL,LTSC,LNSC
450  70  FORMAT (4F(2.6))
460  CLOSE ( UNIT = 2)
470  CALL PI (IO,IPN)
480  NBI=NIE*NBP
490  NEI=NBL/NBP
500  IF (IIP,NE,2) GO TO 77
510  77  WRITE (5,80)
520  80  FORMAT ('$WHICH DRIVE ? ')
530  READ (5,90) IIDR
540  90  FORMAT (7I5)
550  C
560  WRITE (5,100)

```





ORIGINAL PAGE IS  
OF POOR QUALITY

APPLICATIONS DIVISION

```

SEQ      CZSNR,FTN13          26-FEB-81  12146108  PAGE      3
1130      ICMN= IEO+1
1140      ICMX= IEO+NIE
1150      CALL ALTPRT(,40)
1160      C
1170      C
1180      CALL IMOPEN (1,ST,,IIDR,NBI,NIL,'R')
1190      CALL IMOPEN (2,STO,,IODR,NBO,NL,'M')
1200      D      CALL ASSIGN ( 3, 'CZCS3,LST')
1210      C
1220      C
1230      C      WRITE (4,144) XFO,YFO,XSC,YSC
1240      C144  FORMAT( '      XFO          YFO          XSC          YSC '
1250      C      +      ',,4F15.4 )
1260      C      WRITE(4,144) INSKIP,OUTSKIP,NRNMVS,MVTYPE
1270      C144  FORMAT( ' INSKIP  OUTSKIP  NRNMVS  MVTYPE ',,4I8 )
1280      C
1290      C
1300      230  IEC=IBC+NDE-1
1310      IF (IEC.LE,IECC) GO TO 240
1320      IEC=IECC
1330      NOE=IEC-IBC+1
1340      240  NOL=IER-IBR+1
1350      IECP=IEC+1
1360      KO=(IBC-1)*NRP
1370      NO=KO/512
1380      IF(NO,LT,0) NO=0
1390      KO=KO-NO*512
1400      C
1410      C      THESE VALUES ARE SWATH LIMITS
1420      C
1430      DLY = XFO-YSC
1440      DLY = YFO-YSC
1450      XMIN=DLY+(IBC-.5)*DX
1460      XMAX=XMIN+(NOE-1)*DX
1470      YMAX=DLY-(IBR-.5)*DY
1480      YMIN=YMAX-(NOL-1)*DY
1490      C
1500      C      THE 21 TERM POLYNOMIALS DEFINE BOTH U AND V ADJUSTMENTS.
1510      C      SINCE THIS SCHEME WORKS ALONG A SINGLE OUTPUT LINE, THE
1520      C      VERTICAL COMPONENT NEEDS TO BE CHANGED ONLY WHEN A NEW
1530      C      OUTPUT LINE IS CHOSEN. P2 EXTRACTS FROM THE POLYNOMIAL
1540      C      COEFFICIENTS THE HORIZONTAL ADJUSTMENTS, OR SO THE STORY
1550      C      GOES.
1560      C
1570      CALL P2 (XMIN,XMAX,YMAX,Y,DX,DY,DYI)
1580      C
1590      C      WRITE (4,140) XMAX,XMIN,YMAX,YMIN
1600      C140  FORMAT( '      XMAX          XMIN          YMAX          YMIN '
1610      C      +      ',,4F15.4 )
1620      C      WRITE (4,142) DX,DY,DLY,DLY
1630      C142  FORMAT( '      DX          DY          DLY          DLY '
1640      C      +      ',,4F15.4 )
1650      C      WRITE (4,146) TH,Y,DYI
1660      C146  FORMAT( '      TH          Y          DYI          '
1670      C      +      ',,4F15.4 )
1680      C

```





```

SEQ      CZSNR,FTN13      26-FEB-81  12146100  PAGE    5
1.....1.....1.....1.....1.....1.....1.....1.....1.....1.....
2250      255      IF(LC,GT,0) GO TO 256
2260      LC= LC+NSL
2270      GO TO 255
2280      256      CONTINUE
2290      C
2300      START = MAX( 0, CVAL - IEO - ( NBL/NBP ))
2310      NHLTS= START *NBP/512
2320      IF(NHLTS,LT,0) NHLTS=0
2330      IRN=ILN-TLO
2340      IF (IRN,GE,1,AND,IRN,LE,NIL) GO TO 260
2350      CALL MOVE (0,0,LBF,2,1024,2)
2360      GO TO 270
2370      260      CONTINUE
2380      CALL IMSHRT (1,NHLTS,NBTR)
2390      CALL IMREAD (1,IRN,LBF)
2400      270      NBYTES= NHLTS*512
2410      K= START *NBP-NBYTES+1
2420      275      CALL MOVE (LBF(K),1,JBUF(1,LC),1,NBL,0)
2430      C
2440      C      THE INPUT SPACE IS SKEWED IN RELATION TO THE OUTPUT SPACE.
2450      C      THE OFFSETS CALCULATED HERE ALLOW THE INPUT SPACE TO BE STORED
2460      C      AS A RECTANGULAR AREA. WHEN IT IS INDEXED INTO, THE OFFSETS
2470      C      ARE USED TO SELECT THE PROPER AREA.
2480      C
2490      IOFF(LC)= START*NBP
2500      ILN=ILN+1
2510      C      IF (J,EQ,1) KMIN = MIN( START, KMIN )
2520      GO TO 250
2530      C
2540      280      CONTINUE
2550      C
2560      C      GO TO 99901
2570      C
2580      C99901 GO TO I99900,(99903)
2590      C*****
2600      C*****
2610      C
2620      IF(NO*512+NBTH,GT,NBO)NBTH=NBO-NO*512
2630      C
2640      C
2650      CALL IMSHRT (2,NO,NBTH)
2660      CALL IMREAD (2,ORN,LBF)
2670      C
2680      D      IF ( MOD( J-1,50),LE,0) WRITE(4,409A)
2690      04098 FORMAT('1', ' LINE WC ICL NPN WR IRL',
2700      D      +, ' NLN STARTS @ LINE'
2710      D      +, 'T80, ' I, ' K WC LC IOFF(LC) WR')
2720      D      WRITE(4,4099) J,W,C,W,R,I,C,L,I,R,L,N,P,N,N,L,N,S,T,A,R,T,L,C
2730      04099 FORMAT('9I8 ')
2740      KOUT= KO+(NOE-1)*NBP+1
2750      D      IF (MOD(KTIMER,NSL),LT,1) PRNTJB = .TRUE.
2760      D      KTIMER = KTIMER + 1
2770      C
2780      DO 400 I=1,NOE
2790      R= DR(I)
2800      WR= R

```



```

SEQ CZSNR,FTN/3          26-FEB-81  12146108  PAGE 6
1.....1.....1.....1.....1.....1.....1.....1.....1.....
2810 CALL MOVE(0,0,IV,2,NBP,1)
2820 IF(WR,GT,IRMX,OR,WR,LT,IRMN) GO TO 399
2830 D IF(WR,GE,IRMN,AND,WR,LE,IRMX)GO TO 382
2840 D WRITE(4,380) I,WR,IRMN,IRMX
2850 D380 FORMAT(' * ROW VALUE OUT OF BOUNDS : I,WR,IRMN,IRMX ',4I6 )
2860 D GO TO 399
2870 C
2880 382 LC=MOD(WR-1,NSL)+1
2890 C
2900 C=DC(I)
2910 WC=C
2920 C
2930 C
2940 IF(WC,LT,ICMN,OR,WC,GT,ICMX)GO TO 399
2950 D IF(WC,GE,ICMN,AND,WC,LE,ICMX)GO TO 384
2960 D WRITE(4,383) I,WR,ICMN,ICMX
2970 D383 FORMAT(' * COLUMN VALUE OUT OF BOUNDS : I,WC,ICMN,ICMX ',4I6 )
2980 D GO TO 399
2990 C
3000 384 K=WC+NBP-IOFF(LC)+1
3010 C
3020 D375 KDELTA = KPREV - K
3030 C WRITE(4,4095) I,K,WC,LC,IOFF(LC),WR,KDELTA
3040 C4095 FORMAT(TA0,7I7 )
3050 D385 KPREV = K
3060 C
3070 D IF (K,LE,NBL,AND,K,GE,1 ) GO TO 388
3080 C KERRCT = KERRCT + 1
3090 C IF ( MOD( KERRCT,100).GT,10) GO TO 399
3100 D WRITE(4,386) J,I,K,WR,WC,IOFF(LC),LC
3110 D386 FORMAT(' * K OUT OF BOUNDS: OUTROW OUTCOL
3120 D +, *K WR WC IOFF(LC) LC'
3130 D + / 18X,7(16,2X))
3140 D GO TO 399
3150 C
3160 IF(K,GE,NBL)GO TO 399
3170 IF(K,LT,1)GO TO 399
3180 388 CALL MOVE(JBUF(K,LC),INSKIP,IV,OUTSKP,NBRMVS,MVTYPE)
3190 K=K+NBP
3200 C
3210 399 CALL MOVE(IV,INSKIP,LBF(KOUT),OUTSKP,NBRMVS,MVTYPE)
3220 KOUT=KOUT+NBP
3230 C
3240 DO 402 JD=1,5
3250 JP=JD+1
3260 DC(JD)=DC(JD)+DC(JP)
3270 402 DR(JD)=DR(JD)+DR(JP)
3280 C
3290 D IF (.NOT.PRNTJB) GO TO 400
3300 D PRNTJB = .FALSE.
3310 D PRNTHD = .TRUE.
3320 D KMIN = ( IOFF(LC) / NBP ) = 5
3330 D JPLUS = LC + NSL = 1 = NLN
3340 C
3350 D DO 4083 KINDX = LC = NLN + 1 , JPLUS
3360 D KWMC = MOD(KINDEX = 1,NSL) + 1

```

